ORNL-5201

MASTER

Properties of Carbonized and Converted Uranium-Loaded Weak-Acid Resins

G. W. Weber
R. L. Beatty
V. J. Tennery

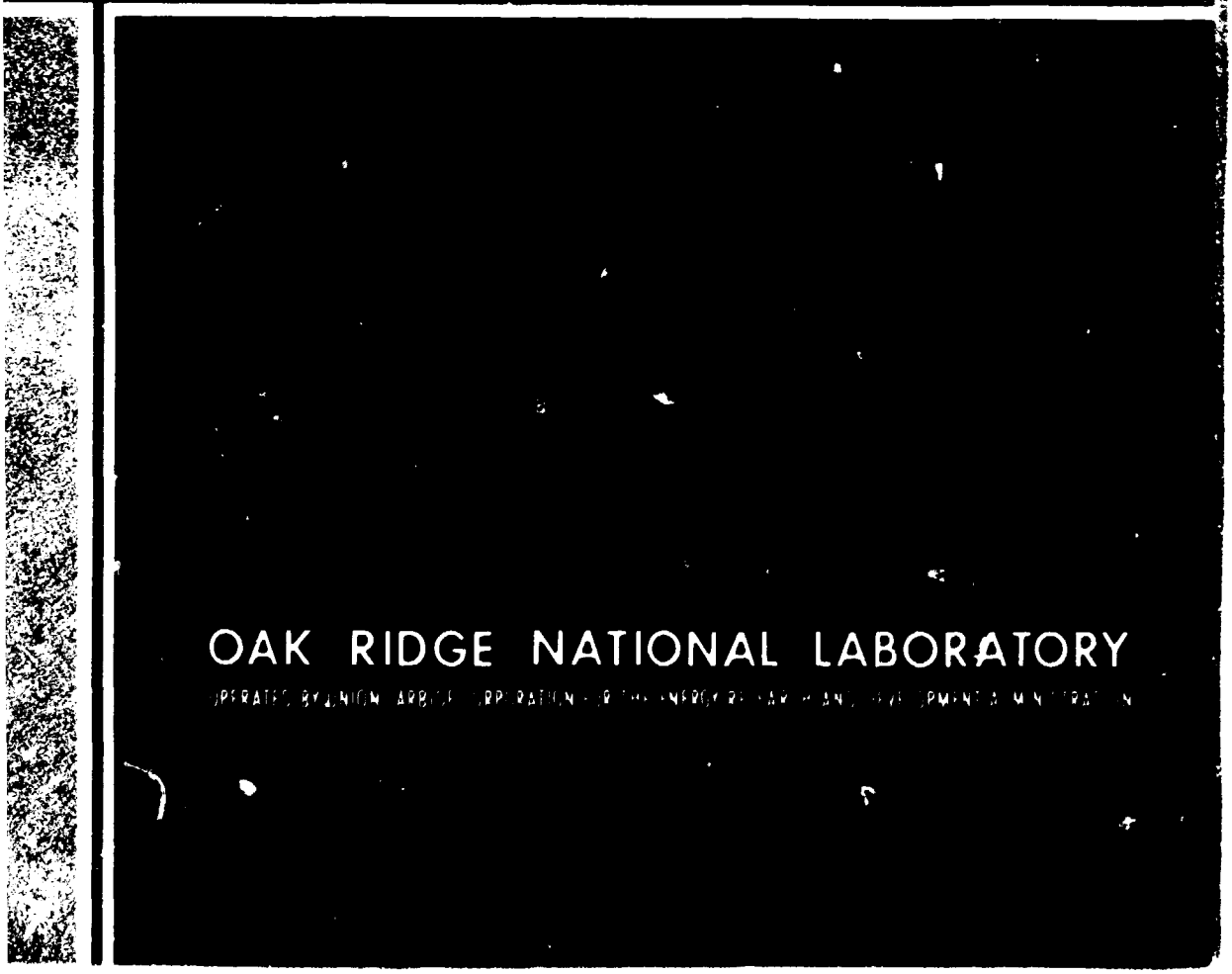

BLANK PAGE

Printed in the United States of America. Available from
National Technical Information Service
U.S. Department of Commerce
5285 Port Royal Road, Springfield, Virginia 22161
Price: Printed Copy $4.50, Microfiche $3.00

ORNL-5201
Distribution
Category UC-77

Contract No. W-7405-eng-26

METALS AND CERAMICS DIVISION

HTGR BASE TECHNOLOGY PROGRAM

Fueled Graphite Development (189a 01330)

PROPERTIES OF CARBONIZED AND CONVERTED URANIUM-LOADED WEAK-ACID RESINS

G. W. Weber
R. L. Beatty
V. J. Tennery

Date Published: February 1977

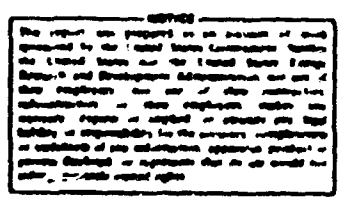

OAK RIDGE NATIONAL LABORATORY
Oak Ridge, Tennessee 37830
operated by
UNION CARBIDE CORPORATION
for the
ENERGY RESEARCH AND DEVELOPMENT ADMINISTRATION

CONTENTS

PROPERTIES OF CARBONIZED AND CONVERTED URANIUM-LOADED WEAK-ACID RESINS

G. W. Weber, R. L. Beatty, and V. J. Tennery

ABSTRACT

Weak-acid ion-exchange resins have been found to provide a practical method for fabricating uranium-containing HTGR fuel kernels. Two steps, thermal decomposition or *carbonization* and carbothermic reduction of UO_2 or *conversion* are required in the manufacture of these kernels.

The properties variations during carbonization of uranium-loaded weak-acid resin-derived fuel proceeds in a manner closely analogous to its thermogravimetric characteristics, particularly the weight loss, volume loss, carbon-to-uranium ratio, density, and particle size. The heating rate through the critical portion of the thermogravimetric curve closely controls the resultant weight loss, volume loss, density, carbon-to-uranium ratio, and subsequent thermal behavior. The optimum carbonization cycle derived discloses a heating rate of 2°C min from 350 to 440°C, and the maximum practicable rate outside of this range.

The conversion of the carbonized material is predictable from classical bulk thermodynamics for removal of carbon monoxide from $UO_2 + C$. Relative phase compositions of UO_2, UC_2, and $UC_{0.9}O_{0.1}$ can be controlled by adjusting conversion conditions. Agglomeration during conversion can be controlled by lowering the carbonization rate and of conversion temperature and increasing gas flow. During this process Duolite C-464 resin appears more resistant to cracking than does Amberlite IRC-72.

INTRODUCTION

The reference fuel kernel for recycle of ^{233}U in high-temperature gas-cooled reactors (HTGRs) is a porous carbon matrix containing finely dispersed UO_2 and or UC_2 derived from weak-acid ion-exchange resin.[1] The process development of this material was begun at ORNL in 1969 and has been in progress since that time.[2-10] The incentives for pursuing the ion-exchange resin route were to take advantage of the commercially available microspheres which could be upgraded to acceptable ranges of size and shape before contact with ^{233}U in a remote refabrication facility, and to develop a fissile kernel having irradiation performance superior to that of other fuels available.

Development of resin-based fuel has included the evaluation of several resin types, effects of varying carbonization cycles, control of conversion (reduction to carbide), plus atmospheric requirements for handling, coating, and process optimization. Both strong- (SAR) and weak-acid (WAR) resins were evaluated for performance and ease of preparation. The SAR-derived material has potential as an advanced fuel because of its excellent thermal stability but is of secondary interest for immediate HTGR application due to the sulfur content.[4,6] Development effort has thus been concentrated on the WAR-based fuel employing acrylic acid-divinylbenzene resins, Amberlite IRC-72, manufactured by Rohm & Haas, and Duolite C-464, manufactured by Diamond Shamrock. The overall process flowsheet is shown in Fig. 1. This report will address the development of the carbonization and conversion (carbothermic reduction) steps starting from the dried uranium-loaded resins.

The two primary process heat-treatment steps are thermal decomposition of the resin, called *carbonization*, which yields UO_2 in an excess of carbon, and carbothermic reduction of the resultant UO_2 to UC_2, called *conversion*. The material is then coated with appropriate pyrolytic carbon and silicon carbide layers designed for optimum irradiation performance.[5,7,9,10]

The as-received material is normally a Na^+-form resin in a hydrated bead supplied in the size range 20 to 30 mesh. This resin was developed as a carboxylic cation exchange resin based on a copolymer of

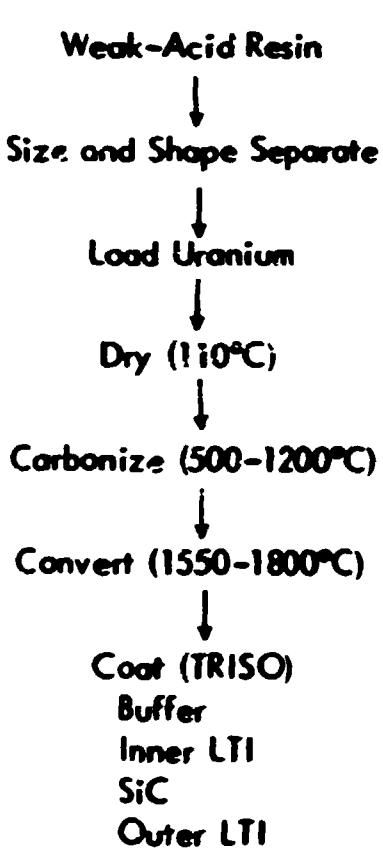

Fig. 1. Preparation of Triso-Coated Resin-Derived Fission Particles.

methacrylic acid and divinyl benzene.[1] By current flowsheets, the material is first converted to a H^+ form, then loaded with uranyl ions by contacting the resin with a uranyl nitrate solution which is acid deficient.[2]

This material is then dried at 110°C to remove some water and yield resin $+UO_2^{++}$. The resultant molecular arrangement is shown (Fig. 2). The approximate IRC-72 kernel diameter at this stage is typically 550 μm with a density of 1.6 g/cm^3, with 47% uranium at a loading of 63 μg/particle.

The carbonization process completes the removal of H_2O and thermally decomposes the resin structure to carbon. This process occurs from drying temperatures up to approximately 900°C, producing UO_2 very finely dispersed in a porous carbon matrix. The resin properties at this stage vary considerably, depending upon the method of carbonization with carbon to uranium ratios of from 4 to 6, a size of approximately 375 μm with a density of 2.4 to 3.7 g/cm^3 and weight percent uranium of 67 to 75%.

The conversion process involves carbothermic reduction of the UO_2 in the carbon matrix to UC_xO_{1-x} and UC_2 by the reaction

$$UO_2 + 3.86\,C \rightarrow UC_{1.86} + 2\,CO$$

and

$$UO_2 + 3\,C \rightarrow UC_xO_{1-x} + (2-x)\,CO.$$

ORNL-DWG 74-2388R

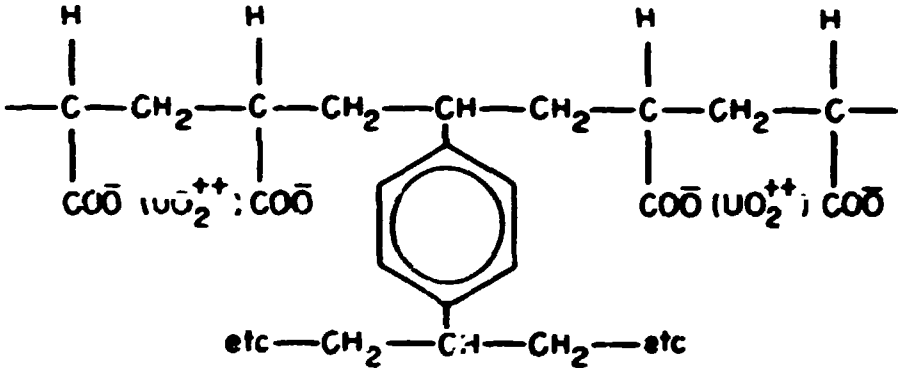

Fig. 2. Uranium-loaded Acrylic Acid–Divinylbenzene Copolymer.

Although UC_2 is the nominal composition, a more correct formula is approximately $UC_{1.86}$. Similarly, there is some question as to whether $UC_{1-x}O_x$ becomes UC as reduction proceeds. The existing thermodynamic data are for the $UO_2 \rightarrow UC$ and $UO_2 \rightarrow UC_2$ reactions however. The degree and manner in which these reactions are carried to completion at 1500 to 1800°C determine the relative proportions of the UO_2, UC_2, and $UC_{1-x}O_x$ phases. The percent oxygen removed from the carbonized material is defined as the percent conversion (UO_2 = 0%, UC_2 = 100%). The calculated variation of the partial pressure of the carbon monoxide (Fig. 3) for the two principal conversion reactions controls the extent and rate to which conversion is carried out.[1,2] This is true because of the very high surface areas present in the carbonized material (100 m^2/gm) and the availability of an excess of finely dispersed carbon. Thus, at a given temperature, the reduction rate is controlled by the specific argon flow rate (system at 1 atm). Calculated reduction rates at various temperatures are shown (Fig. 4) normalized to 0.05 liter/min of sweep gas per gram uranium; the argon flow rate is directly proportional to the reduction rate. Of course, selection of flow rate is limited to a range suitable for fluidization. Essentially complete reduction can be effected in a few minutes at 1800°C, and controlled partial reduction may conveniently be done in the 1600 to 1700°C range (Fig. 4). However, it should be emphasized that the linear reduction data (Fig. 4) apply only as long as the material has sufficient open porosity (i.e., does not sinter appreciably).

The final weight percent uranium ranges from 72 to 86%, depending upon the conversion process. Final density ranges from 3.2 to 6 g/cm^3, with an average microsphere diameter of 360 μm for Amberlite IRC-72.

The prepared fuel kernels are then given a low-density pyrolytic carbon (PyC) buffer coating, a high-density PyC isotropic coating, a silicon carbide coating, and another high-density PyC isotropic coating to yield a finished TRISO HTGR fissile particle.

The current work examines four aspects of carbonization and conversion:

1. the effect of heating rate at various stages of the carbonization cycle on the final carbon-to-uranium ratio, weight loss, volume loss, surface area, and subsequent conversion behavior;
2. the variation during the carbonization and conversion cycles of the density, pore size distribution, surface area, weight loss, volume loss, and carbon-to-uranium ratio;
3. the effect of different conversion temperatures and atmospheres on the proportions of UO_2, $UC_{1-x}O_x$, and UC_2 in the final material; and

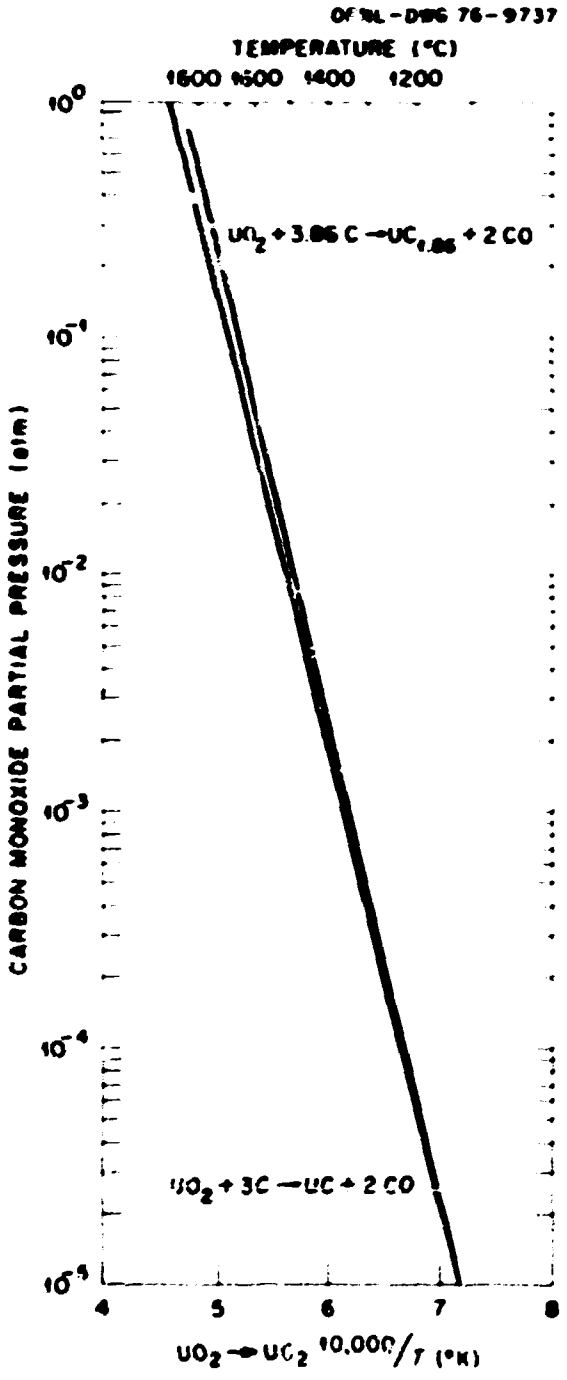

Fig. 3. Variation in Partial Pressure of Carbon Monoxide with Temperature for Conversion of UO_2 to UC_2 by Two Different Reactions.

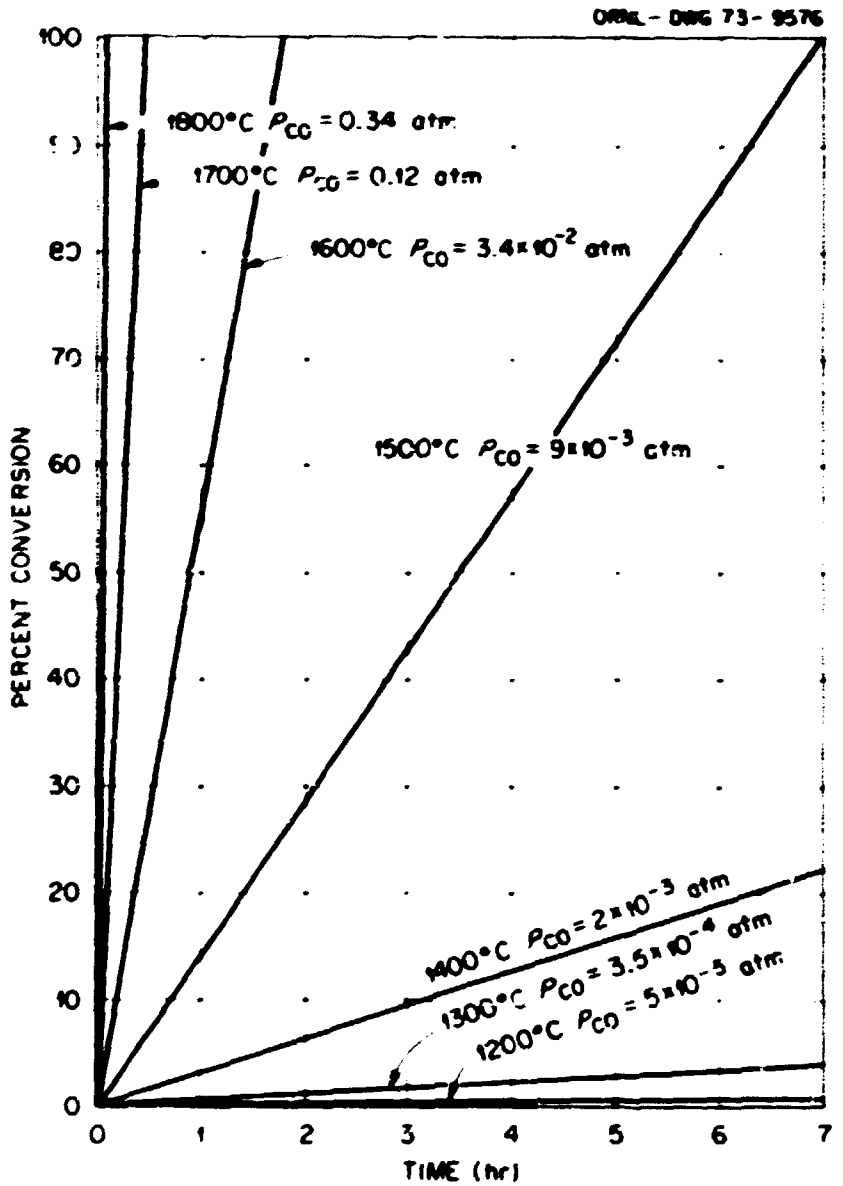

Fig. 4. Fluidized Bed Conversion of Uranium-Loaded Weak Acid Resin from Oxide to Carbide. (Assumed Equilibrium P_{CO} for Reaction UO_2 + [illegible] + 2CO. Normalized to 0.05 Liter/Min of Sweep Gas per g of Uranium).

4 the correlation between the observed conversion rate and the behavior predicted from classical bulk thermodynamics.

EXPERIMENTAL PROCEDURE

Material and Furnaces

The carbonization, conversion and coating steps were done in vertical graphite resistance furnaces (Fig. 5). The graphite coating chamber consists of a cone with an included angle of 36 or 60° fixed or machined to a cylindrical graphite piece. The nominal coating chamber diameter is 2 1/2 in., with diameters of 3/4, 1, 1 3/8, and 1 3/4 in. also available with appropriate adapters. Two methods of temperature

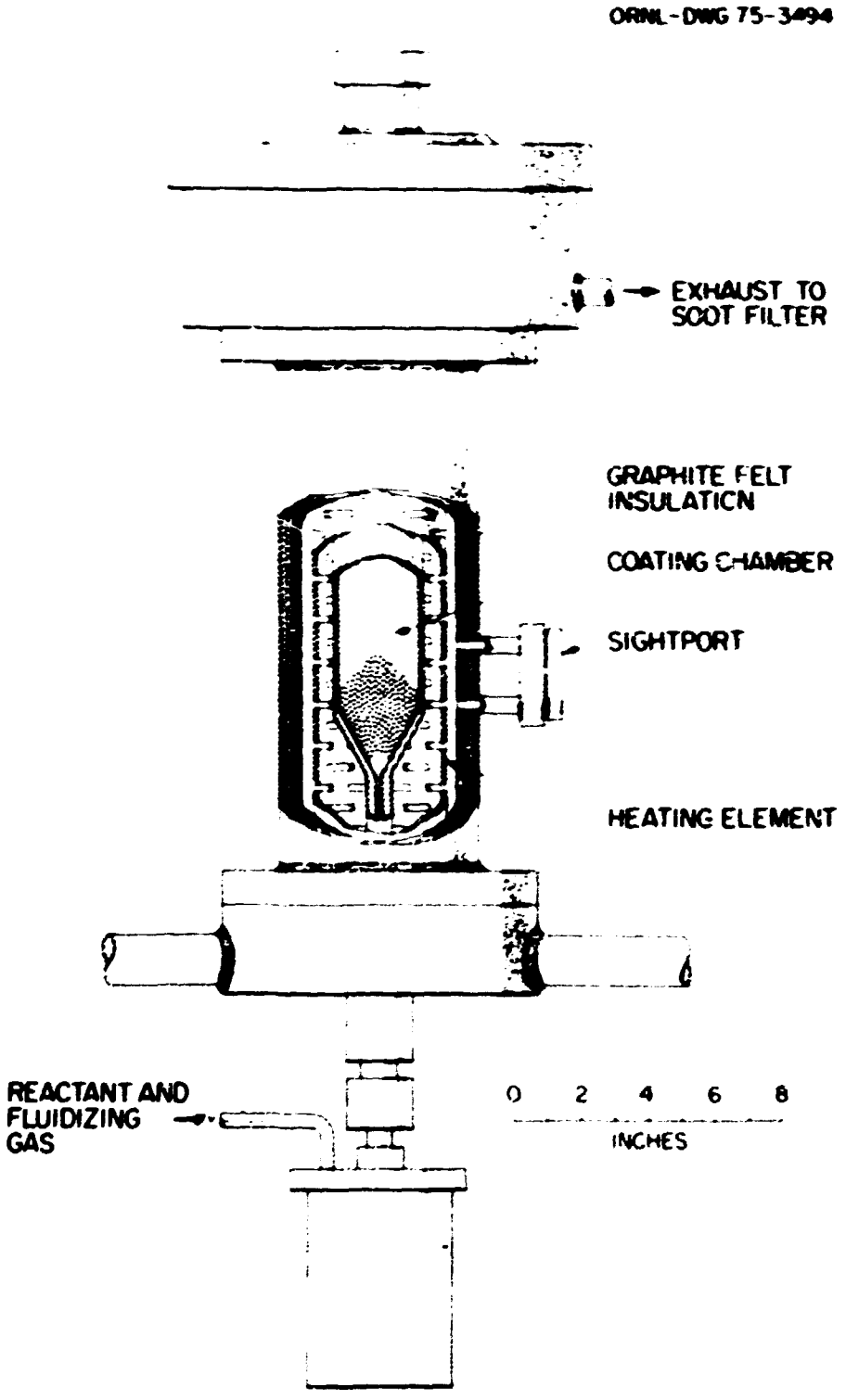

Fig. 5. Particle-Coating Furnace Used for Carbonization, Conversion and Coating of Weak-Acid Resin-Derived HTGR Fuel Particles.

measurement are available. A sheathed Chromel-P Alumel thermocouple is inserted directly into the bed through the furnace top for measurement of temperatures from room to approximately 700°C. A sight port is provided for optical pyrometer sighting on the furnace side. The heating element and graphite felt insulation are split to permit direct viewing of the fluidizing chamber wall. Two sight holes are available with the lower one situated just above the cone-cylinder junction. The lower sight port was used throughout this study for measuring temperatures from 800 to 1800°C.

Required fluidizing and reactant gases are supplied through calibrated flowmeters which monitor and control flows from tens of centimeters per minute to tens of liters per minute. Unless otherwise specified, the fluidizing gas used in the carbonization and conversion experiments was high-purity argon.

Program control of furnace operation to 600°C was effected with either a cam-operated Trendtrac controller using feedback from a Chromel-P Alumel thermocouple or a nonfeedback pulse interval timer controlling the power supply. Furnace control above 600°C was accomplished manually.

The material studied was Amberlite IRC-72 resin (made by Rohm & Haas, Philadelphia, Pennsylvania) and Duolite C-464 (made by Diamond Shamrock Chemical Company, Redwood City, California). Both resins are possible alternate sources and were compared directly when appropriate.

Thermogravimetric Analysis

As thermal decomposition and water removal from the resin are accompanied by substantial weight loss, thermogravimetric analyses (TGA) identified critical carbonization temperatures. Different heating rates were used in the TGA work to determine the effect of different carbonization rates on the decomposition of the resin. Dried resin was analyzed with a Mettler Recording Vacuum Thermoanalyzer using 150 mg samples in a flowing argon atmosphere. Temperatures were measured with a platinum vs Pt - 10% Rh thermocouple. The sample holder was an 8- × 20-mm-platinum crucible with a platinum lid.

Differential Thermal Analysis

Since resin decomposition is accompanied by significant thermal effects,[3,4] differential thermal analysis (DTA) measurements were conducted to better define critical reaction steps. These measurements were made with the Mettler thermoanalyzer simultaneously with the TGA measurements. The reference material was Al_2O_3 powder with a sample weight equal to that of the dried resin sample. The sensitivity and time response of the DTA instrument were such that optimum DTA traces were obtained only at a heating rate of 5–7°C/min.

An experiment determined the species that evolved at different temperatures. Fifty grams of resin were heated at 5°C/min in a 1-in.-diam coating tube with a 2 liters/min argon flow. The off-gas was collected at 150, 250, 355, 425, 475, and 600°C in a series of parallel sampling bottles by sequential bottle isolation at each stated resin temperature. The contents of these bottles were then analyzed by gas chromatography. An in-line water-cooled trap was installed to monitor evolution of condensables.

Effect of Heating Rate During Carbonization

The TGA and DTA results showed the special importance of the range from room temperature to 500°C as regards weight loss and thermal behavior in the carbonization cycle. To determine the effect of heating rate on critical process parameters, U-loaded 25 +30 mesh Amberlite IRC-72 batches were heated at different rates from room temperature to 500°C followed by rapid heating to 1200°C. Batches of 25.0 g were heated in 1-in.-diam tubes with a fluidizing gas flow of 3 liters/min to 500°C and then 2 liters/min to 1200°C. After heating at 1200°C for 5 min, the samples were analyzed for weight loss, volume loss, and chemical composition.

To further define the region of importance in carbonization, similar experiments were done with Duolite C-464 resin. Material of −30 +35 mesh in batch sizes of approximately 40 g was heated in a 1 3/8 in. furnace tube. Heating rate was planned to yield various heating curves. Gas flow was regulated during the run at 9 liters/min from room temperature to 100°C, 8 liters/min to 200°C and 6 liters/min to 600°C. The final temperature of 1200°C was held for 30 min. Weight loss, volume loss, and chemical composition were determined for the carbonized material.

Change in Properties During Carbonization

The physical property variations with temperature during a typical carbonization run were determined with tests on Duolite and Amberlite. Batches of 70 g were heated in a 1 3/8-in.-diam tube at 2°C/min to selected temperatures under 500°C and at 20°C/min to temperatures over 500°C and then cooled rapidly to room temperature. Fluidizing gas flows were 15 liters/min from room temperature to 185°C, 9 liters/min from 185 to 950°C, 7 liters/min from 950 to 1200°C, and 4 liters/min from 1200 to 1625°C. Weight loss, volume loss, tap density, mercury density, mercury porosimetry, BET surface area, carbon-to-uranium ratio, and particle size were determined. Tap density as discussed in this report is the weight of particles divided by the volume occupied in a graduate of appropriate size, assuming perfect packing; tap density/0.62 is equal to the true pens. As temperature increases, the finely distributed UO_2 agglomerates into coherently diffracting regions of increasing particle size. To investigate this behavior, samples were heated to different temperatures in the carbonization cycle, rapidly cooled to room temperature, and examined by x-ray diffraction. The material was ground in a Diamond Plattner mortar to −325 mesh and sealed in 0.005-in. glass capillaries with Apiezon and household cement. The sample was examined with an 11.54-cm-diam Debye-Scherrer camera with monochromatic CuK_α x rays for approximately 46 hr.

Other Carbonization Process Parameters and Uranium Loss

Uranium loss during carbonization was determined with an improvised collecting scheme. Because the uranium-containing species released during carbonization may be carried in an aerosol, collection is difficult. The collection method involved packing the furnace lid and initial off-gas flow path with gauze. After a run, the gauze and a newly constructed and therefore previously uncontaminated furnace lid were counted with an alpha survey meter. The tars and residue in the gauze were to function as a collection medium for the aerosols given off during carbonization; but how successful this was is not known. A typical carbonization cycle was run with 235 g of material at 2°C/min to 1200°C.

A second cycle was run in which a 150-g batch was heated from room temperature to 1200°C at approximately 170°C/min. The residue collected on the top portions of the furnace was absorbed on tissues and gauze and sprayed with acetone to break down the tars for alpha counting. The tissues and gauze were subsequently reduced to ash and the uranium content determined.

Alternate carbonization atmospheres were investigated in an attempt to increase the resin coking yield (carbon-to-uranium ratio). As this process of thermally decomposing the resin is similar to pyrolysis reactions in other hydrocarbons, alternative approaches suggested by such work were explored. Bacon[13] has shown that substituting hydrogen chloride for nitrogen significantly decreased the weight loss and widened the temperature range of reaction for the pyrolysis of rayon. Similarly, substituting oxygen for argon up to the critical reaction temperature decreased the weight loss observed in pyrolysis of Villwyte rayon.

To investigate atmospheric effects on the HTGR resin process, air was substituted for argon to 270°C, the point of the first significant reaction, in a 1200°C carbonization process for a 40-g batch of Amberlite IRC-72 resin heated at 2°C/min. Carbon and uranium content were determined for the resultant material.

Similarly, the effect of hydrogen chloride was investigated by installing a bubbler with concentrated hydrogen chloride in the fluidizing gas (argon) line. Hydrogen chloride was introduced to 500°C in runs otherwise identical with those previously described.

Exposure experiments on these materials were done also to determine what effect the different procedures might have on the reactivity of the carbonized material. One-gram batches of the carbonized material were exposed to air and the resultant weight gain recorded.

Change in Properties During Conversion

To ascertain the property variation during the conversion process, a series of 70-g batches of Amerlite and Duolite was carbonized in a 1 3/8-in.-diam tube at 2°C/min to 500°C, 20°C/min from 500 to 1200°C, and 100°C/min from 1200 to 1625°C. The fluidizing gas flows were 15 liters/min from room temperature to 185°C, 9 liters/min from 185 to 950°C, 7 liters/min from 950 to 1200°C, and 4 liters/min from 1200 to 1625°C. The percent weight loss, percent volume loss, particle size, tap density, mercury density, and carbon-to-uranium ratios were determined as a function of time at conversion temperature. Times from 0 min to 1.67 of the time calculated for complete conversion of the UO_2 to UC_2 were used.

The pore size distribution produced in partially converted weak-acid resin Duolite and Amberlite fuels was studied by carbonizing and converting batches containing 120 g of uranium at 1525°C to 34 and 32% conversion respectively. The pore size distribution of this material was then determined by measuring the mercury density as a function of pressure. The diameter of the pores penetrated by mercury was determined from the formula:

$$\text{diam } (\mu\text{m}) = \frac{175}{\text{psia (Hg)}}$$

Conversion Rate and Thermodynamics

Experiments were also conducted to directly compare observed with predicted conversion levels for various specific gas flows, temperatures, and batch sizes. Thirty-five experiments were conducted at gas flows from 0.295 to 7.37 liters of argon/gram of uranium at temperatures from 1500 to 1690°C and at conversion levels from 15 to 93%. Batch sizes varied from 28 to 486 g in furnace tubes from 3.5 to 10.8 cm in diameter. Five of the experiments were conducted with Duolite C-464 and the other 30 with Amberlite IRC-72. Additionally, particle size was varied for different batch sizes and gas flows to ascertain the effect on conversion level for a series of six different runs at 1575°C in a 4.44-cm-diam tube.

To ascertain the possible temperature error between measured and actual temperature during a conversion run, parallel measurements were carried out with a platinum vs Pt–10% Rh thermocouple in the bed and an optical pyrometer sighting on the furnace tube wall (Fig. 5). The bed thermocouple and top sighting port were located 7.3 cm above the tube orifice. The normal measuring sight port used for experimental control is 3.5 cm above the tube orifice. The particle bed extended to approximately 8.6 cm.

To investigate the effect of fluidization conditions, the platinum vs Pt–10% Rh bed thermocouple and control sight port were simultaneously monitored at approximately constant power level as fluidization conditions were varied.

Product Phase Evaluation

Phase identification studies were conducted by carbonizing material at 2°C/min to 600°C and then heating to the conversion temperature. Conversion was done at 1505 and 1625°C in argon; at 1625°C in

argon with 4% hydrogen addition and at 1628°C in argon with carbon monoxide addition equal to 0.75 of the equilibrium partial pressure of carbon monoxide at the conversion temperature. To accomplish this last addition, carbon monoxide was added to the fluidizing. After conversion, this material was analyzed for phase content by the x-ray power technique described previously of the gas in proportion to 0.75 partial pressure at 1628°C.

Uranium Loss During Conversion

To identify the amount of uranium lost during the conversion process, a water-cooled aluminum furnace probe was fabricated to condense and quantitatively collect any uranium released during the process. This probe extended downward to a point immediately above the hot zone of the furnace (Fig. 5) to ensure complete condensation and collection of uranium-bearing vapors. A run with 150 g of carbonized, screened, shape-separation rejected kernels was made to 73% conversion at temperatures from 1650 to 1800°C. After the conversion the furnace probe was counted with an alpha survey meter. A 5% solution of nitric acid was used to remove the collected material from the probe for chemical analysis.

A similar run was made with 150 g of shape-separated, screened carbonized (2°C/min) material to approximately 98% conversion at 1775°C. Throughout this run, the furnace probe was subjected to direct particle impingement so that particles actually stuck to the probe. Loose particles were removed and the probe counted with an alpha survey meter.

Fluidization Control During Conversion

Investigations were made of the critical process parameters affecting bed sticking or agglomeration during conversion of weak-acid resin-derived fuel. A single lot of dried Amberlite IRC-72 resin was carbonized at 2°C/min from 200 to 500°C and then at 20°C/min to 1200°C in two batches of 1000 and 730 g. The material was then converted in a 4.44-cm-diam tube at 1525°C in 80 g batches at argon flows from 4.5 to 9.0 liters/min. Final kernel diameter was 450 μm with a density of approximately 3.1 g/cm^3.

Since the onset of bed sticking is not easily specified, a subjective classification was established. A Magnehelic gage, installed to measure injector back-pressure, was used for the arbitrary classification. The bed was categorized as *free* if Magnehelic pressure variation was less than 5 cm of water, showing "slight slugging" if pressure cycling was 12.5 cm or less, "heavy slugging" if the cycling was greater than 12.5 cm, and "sticking" if the gage went full scale (125 cm) twice or failed to recover after the first excursion. Slugging is a visually observable phenomena in which the material settles and is then blown in a mass up into the furnace tube. The time at which this occured was recorded, and assuming a constant conversion rate with time, the approximate conversion level at which this behavior occurred was determined. The gas flow for each run was divided by the total bed particle area to establish a gas flux.

To evaluate the relative agglomeration behavior of the two candidate resins, a comparison run was made in a 1-in. tube at 2.5 liters/min argon with 50-g batches of dried resin. A heating rate of 8°C/min from 100 to 500°C and a conversion time of 30 min at 1700°C were used. The Duolite batch was very loose throughout while the Amberlite nearly stuck at 12 min into the run and barely remained fluidized for the remainder of the run.

Analagous runs were made with 80 g of material in a 1 3/8 in. tube at 2.5 liters/min. The Amberlite run was aborted after 11 min at 1700°C due to sticking and slugging of the batch. The Duolite run was completed without incident.

Larger comparison runs were made with approximately 250 g of material in a 2 1/2 in. tube at 5.0 liters/min. Conversion was done at 1625°C for 33 min. The Duolite resin was slightly sluggish the last 6 min of the run. However, the Amberlite became sluggish 3 min into the run and began sticking 5 min into the run.

Atmospheric Reactivity

To compare carbonized particle-atmosphere reactivities as a function of heat treatment, lots from a single batch of loaded IRC-72 were heated to 600, 1200, and 1600°C respectively and exposed to room atmosphere. The 1200°C treated particles were fully carbonized, with the contained uranium being essentially UO_2. The 1600°C treated particles were nominally UO_2 + C with about 15% of the oxygen removed. Duplicate 1-g samples, one each in an uncapped bottle initially filled with argon and the other poured into an open beaker, were exposed to compare reaction rates.

In a further experiment, weight gains were recorded as functions of time for uranium-loaded IRC-72 treated at 500, 1200, and 1800°C; these samples were respectively: carbonized through the critical heating rate range; fully carbonized; and fully reduced to dicarbide.

RESULTS

Thermogravimetric Analysis

The thermogravimetric analyses (TGA) showed Amberlite IRC-72 material experiencing a gradual weight loss to 270°C for the 2°C/min heating rate (Fig. 6). The 2°C/min rate then shows a larger weight loss to 315°C followed by a large weight loss from 360 to 440°C. Above 480°C, little weight loss occurs to 1000°C. Increasing the heating rate to 6°C/min causes an apparent delay in the first loss to about 315°C which continues to approximately 360°C. The large weight loss at 6°C/min occurs from 395 to 485°C followed again by little loss to 1000°C. This shift of weight loss to higher temperatures with increasing heating rate may be attributed to lag in the response of the measuring apparatus. It is also apparent from the final weights that faster heating rates produce more weight loss.

The Duolite C-464 resin showed essentially no weight loss to 210°C, after which a gradual loss occurred for all heating rates. Faster weight losses occurred with lower heating rate to about 315°C above which weight loss accelerated. The largest weight loss occurred for the 2°C/min heating rate from 375 to 460°C, for the 6°C/min heating rate from 390 to 480°C, and for the 10°C/min heating rate from 405 to 500°C. Above these maximum temperatures little additional weight loss occurs to 1000°C. It is apparent that, for a given heating rate, Duolite C-464 resin requires higher temperatures than does Amberlite IRC-72 to produce equivalent resin breakdown. That most weight loss occurs in the one narrow range from about 350 to 450°C is apparent from all of the TGA results obtained.

Differential Thermal Analysis

The differential thermal analysis for the Duolite C-464 and Amberlite IRC-72 shows three broad endotherms for both resins (Fig. 7). The Amberlite shows negative peaks at 160–220, 330, and 490°C. Comparison of these peaks with the 6°C/min TGA results shows that the first broad peak corresponds closely with the initial gradual weight loss. The second large endotherm from 280°C to a peak at 330°C matches very closely the accelerating weight loss shown on the TGA curve. The largest endotherm beginning at 415°C and peaking at 495°C may correspond as well to the observed weight loss curve. The relative DTA peak sizes likewise are in accordance with their relative weight losses. These DTA results correspond in peak temperatures to the results of Pollock and Silverman[4] if endotherms are tabulated. The two apparent exotherms at 290 and 420°C may be caused by a shift in the base line since exothermic behavior is not expected in a destructive distillation process. The occurrence above 500°C of a steadily decreasing exotherm may possibly be due to evolution of hydrogen.

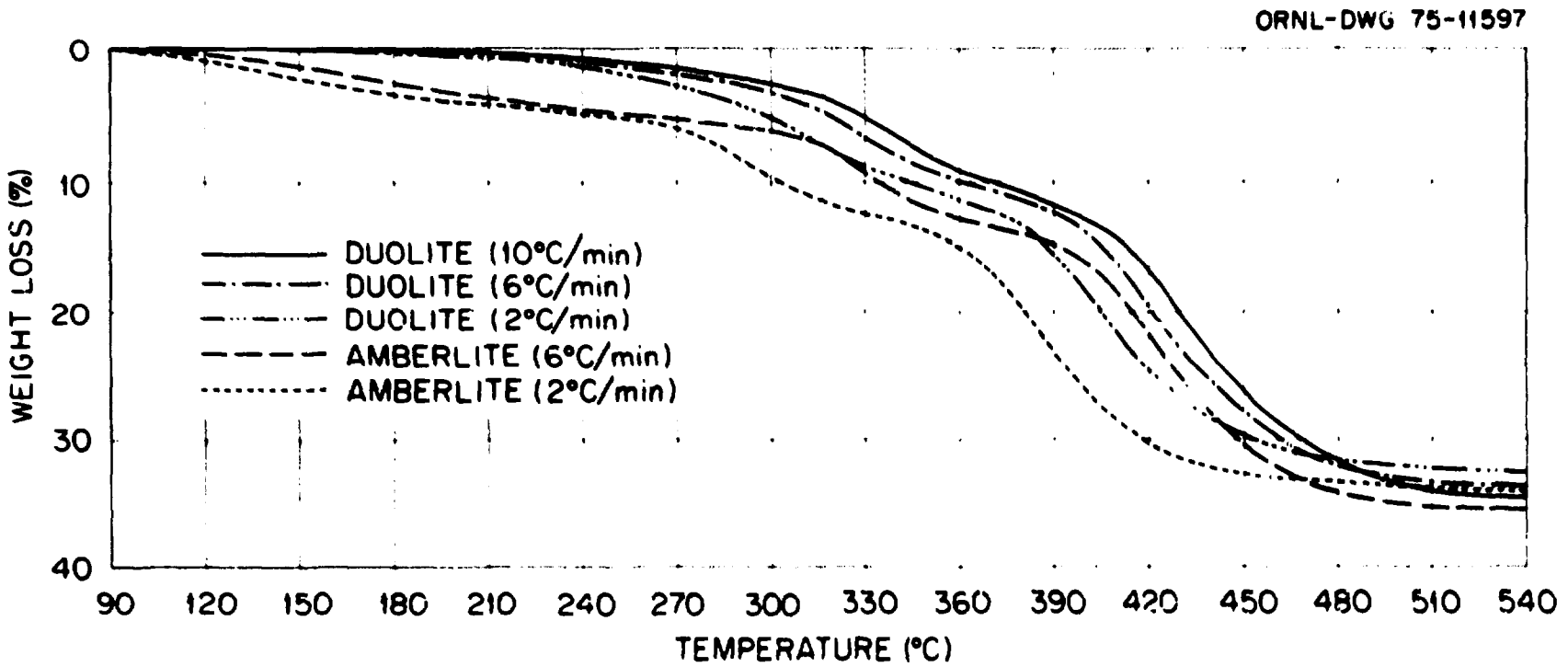

Fig. 6. Weight Loss of Uranium-Loaded Duolite (C-464) and Amberlite (IRC-72) Weak-Acid Resins from 90 to 540 C as a Function of Temperature.

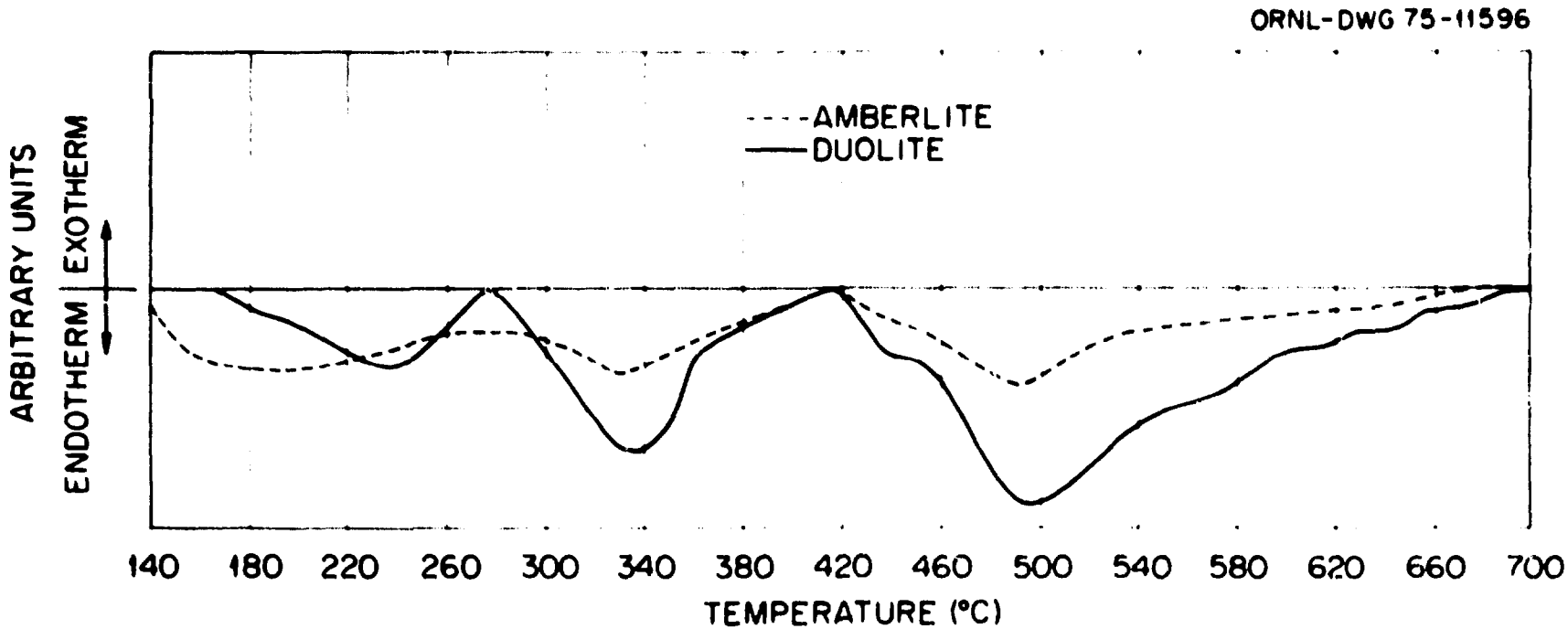

Fig. 7. Differential Thermal Analysis Behavior of Uranium-Loaded Duolite (C-464) and Amberlite (IRC-72) Weak-Acid Resins Heated at 6°C/Min.

The DTA results for Duolite shows peaks at 240, 335, and 480 C. The two higher peak temperatures correspond closely to those observed for Amberlite, indicating that similar processes may be occurring in both resins above 270°C. These two peaks correspond closely to the two largest weight loss portions of the TGA curves. There is no deflection in the TGA curve corresponding to the 240 C peak. However, this temperature does represent the point at which weight loss begins to occur for the C-464 material. This suggests that the weight loss associated with the second peak may be superimposed to such an extent that resolution of the discrete weight loss behavior of the first TGA event may be impossible under the current experimental conditions. Another possible explanation might be a nonvolatilizing reaction like a phase change. Little study of the nature of the species involved in the destructive distillation process in each temperature region has been done. Pollock and Silverman[4] heated separate samples of Amberlite resin and passed the gaseous products through a gas chromatograph. Water, carbon monoxide, carbon dioxide, and mixtures of light unsaturated hydrocarbons were detected. The gas chromatographic observation of samples collected in the current study during a carbonization run indicated that condensables were formed at approximately 170°C. No real accumulation was observed from this temperature until 475 C when traces were formed in the trap. Also large amounts of smoke, first observed at 355°C, continued to evolve heavily to 475°C but essentially disappeared by 500°C. Some aromatic tarlike components condensed readily at 425°C. The only exhaust line temperature increase (at approximately 300°C) indicated a large increase in gas evolution. These qualitative observations are in good agreement with the expected behavior from the TGA. The major weight-loss reaction occurring from 350 to 480°C in the TGA is accompanied by considerable evolution of dense smoke and some condensable tars. The condensable formed at low temperatures is probably water from the lowest temperature endothermic peak.

The chromatographic analyses in the current study indicated that at 425°C the off-gas contained (in mole %) 0.55% CO, 0.2% CO_2, and the following aliphatic hydrocarbons: C_1 0.452%, C_2 0.160%, C_3 0.068%, normal C_4 0.02%, iso-C_4 0.002%, normal C_5 0.004%, and iso-C_5 0.061%. At 475 C there were 0.46% CO, a trace of carbon dioxide, and hydrocarbons: C_1 0.38%, C_2 0.048%, C_3 0.007%, normal C_4 0.015%, iso-C_4 0.001%, and iso-C_5 0.008% were found. At 600°C, 0.82% CO, insignificant amounts of carbon dioxide and 0.26% of C_1 hydrocarbons were found. The amount of carbon monoxide is nearly constant from 475 to 600°C while carbon dioxide decreases rapidly. The clear tendency is to go to lower hydrocarbons with increasing temperature. The large weight losses occurring from 360 to 480°C thus include mixtures of C_1 to C_5 hydrocarbons and relatively nonvolatile light-to-intermediate aromatics in addition to carbon monoxide and carbon dioxide.

Effect of Heating Rate During Carbonization

Since large amounts of volatiles are evolved during the resin carbonization, an early need was to establish a heating rate limit below which microsphere integrity would not be destroyed. Since initial experiments with programmed heating rates up to 40°C/min through the carbonization range showed no effect of rate on structural integrity, heating rates were increased by loading dried resin into a preheated furnace.

When poured into a fluidizing tube preheated to 600°C, the dried microspheres, due to their significant heat capacity, were heated through the entire range from room temperature to 1200°C at a rate of 200 to 300°C/min and survived intact; they disintegrated when poured into a tube preheated to 1200°C which heated them at a rate between 500 and 1000°C/min. Thus a limit was reached in the heating rate which could be tolerated by a 500-μm dried uranium-loaded WAR microsphere (380-μm after carbonization), but this limit was so high that carefully programmed heating was unnecessary for retaining structural integrity. However, the amount of retained carbon (resin coking yield) was sensitive to the heating rate through a limited critical temperature range.

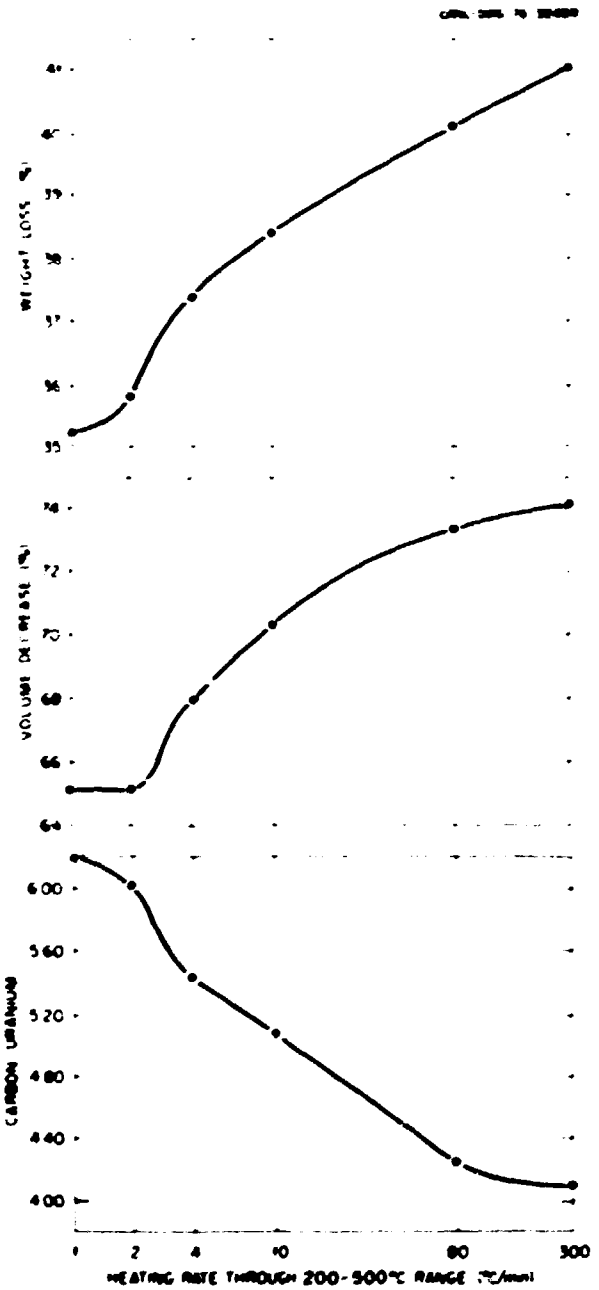

Fig. 8. Effect of Critical Range (200–500°C) Heating Rate on Carbonization of Uranium-Loaded Weak-Acid Resin (Amberlite IRC-72) Carbonized to 1200°C.

The effect of the heating rate on Amberlite IRC-72 from 200 to 500°C (Fig. 8) shows a close correspondence between weight and volume loss* and the logorithm of the heating rate. Chemical analysis of the carbon and uranium indicated a similar strong dependence of the carbon-to-uranium ratio on the logarithm of the heating rate through the critical region (Fig. 8). The nominal amount of excess carbon

*The weight loss observed in this instance is from 35 to 41% with a volume loss of 65 to 74%, from the loaded dried resin.

required to complete the carbothermic reduction during conversion is a carbon-to-uranium ratio of 4. Any heating rate technically feasible will yield a carbon-to-uranium ratio greater than 4. Throughout this range of heating rates, the particles remained intact.

A comparison heating curve in which a very rapid heatup (51 °C/min) to 360 °C was followed with a slow rate (1.43°C/min) from 200 to 500°C and a subsequently rapid completion of the carbonization to 1200°C at a high rate yielded a weight loss of 35.3% and a volume loss of 66.2%. These values agree closely with other results (Fig. 8) if the 360 to 440°C range rate alone is used, this agreement illustrates the critical importance of this very limited processing temperature region in controlling product properties.

The weight losses for different heating cycles for Duolite C-464 (Fig. 9) show that the two curves yielding 32.1% weight loss require markedly different times to reach 600 °C. Although the weight losses for the two runs were identical, the time required to complete the heating to 600°C is over 4 hr in one case and is approximately 1 hr 40 min in the other.

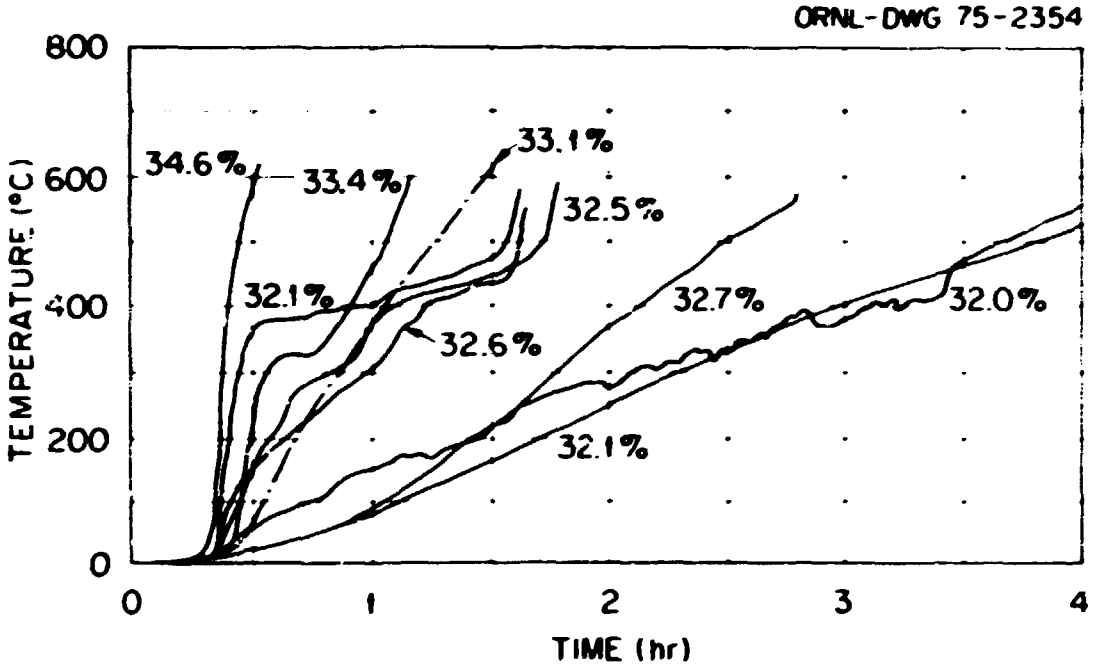

Fig. 9. Percent Weight Loss at Different Heating Rates for the Region from 25 to 600°C During Carbonization to 1200°C of Dried (110°C) Uranium-Loaded Weak-Acid (Duolite C-464) Resin.

To delineate that portion of the curve which exerted the largest effect on the measured parameters, the individual heating curves were broken into three temperature ranges: 160–270°C, 270–360°C, and 360–440°C (Table 1).

There is a close correlation between heating rates through the 360–440°C region and the weight and volume losses. To lend some quantitative support to this correlation, a computer program for a least squares fit with the exponential $y = ae^{bx}$ was used with a Wang 600. Several different programs were evaluated, including $y = ax^b$, $y = ab^x$, and $y = a + bx + cx^2$, but $y = ae^{bx}$ was found to be most satisfactory (Table 2).

The weighting factors for the adjusted rates are based on the normalized relative sizes of the weight losses indicated by that portion of the TGA curve (Fig. 10). It is apparent that the strongest correlation lies with the 360–440°C rate. Two different best fit lines are possible, a lower one for constant heating curves and a slightly higher one for heating curves with very different heating rates in different temperature regions (Fig. 10). Calculation of individual correlation coefficients yielded a value of 0.9995 for the former and 0.9978 for the latter.

Table 1. Property variation as a function of heating rate during carbonization for Amberlite resin

Weight loss (%)	Tap density (g/cm^3)	Volume loss (%)	Heating rate (°C/min) by temperature range (°C)		
			160–270	270–360	360–440
32.0	1.475	60.4	2.44	2.00	1.33
32.1	1.465	59.8	44.0	19.0	1.41
32.1	1.440	59.4	2.83	2.47	1.94
32.5	1.482	60.2	10.17	4.72	2.39
32.6	1.497	61.1	5.00	5.20	2.88
32.7	1.491	60.6	4.67	4.67	4.27
33.1	1.494	61.3	8.56	8.50	8.00
33.4	1.508	61.8	37.33	4.67	9.67
34.6	1.580	64.0	71.33	62.67	62.7

Table 2. The relationship of heating rate to weight loss for uranium-loaded, weak-acid resin

Region	$y = ae^{bx}$ correlation coefficient to weight loss
160–270°C	0.665
270–360°C	0.713
360–440°C	0.994
The two upper regions combined[a]	0.914
All three regions combined[b]	0.873

$$^{a}\text{Rate} = \frac{(270\text{–}360^{\circ}\text{C rate} \times 2.75) + (360\text{–}440^{\circ}\text{C rate})}{8.75}$$

$$^{b}\text{Rate} = \frac{(1 \times 160\text{–}270^{\circ}\text{C}) + (2.75 \times 270\text{–}360^{\circ}\text{C rate}) + (360\text{–}440^{\circ}\text{C rate})}{9.75}$$

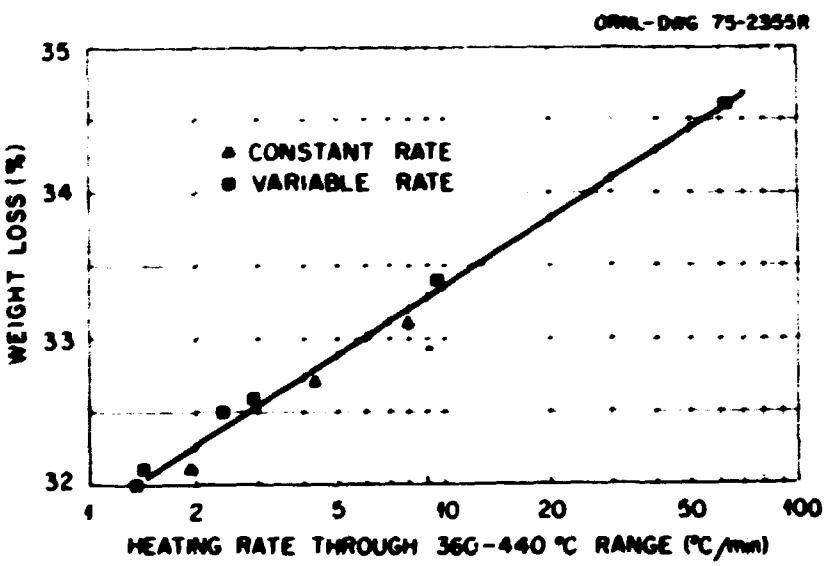

Fig. 10. Weight Loss of Dried (110°C) Uranium-Loaded Weak-Acid (Duolite C-464) Resin During Carbonization to 1200°C as a Function of Critical Range Heating Rate.

A *t*-test for $\rho = 0$ significance was run with a Wang 600 program between the natural logarithmic heating rate and the percent weight loss:

Heating rates	*t* Value	for $n = 2$ *t* Value for 0.001
Constant	72.41	31.60
Variable	26.28	12.94
All	23.58	5.40

This indicates some slight difference in the two situations. However, the difference is small enough that it does not warrant further investigation.

Similar analyses of the volume loss (Fig. 11) and tap density values yielded correlation coefficients of 0.946 and 0.905 for the 360–440°C region respectively.

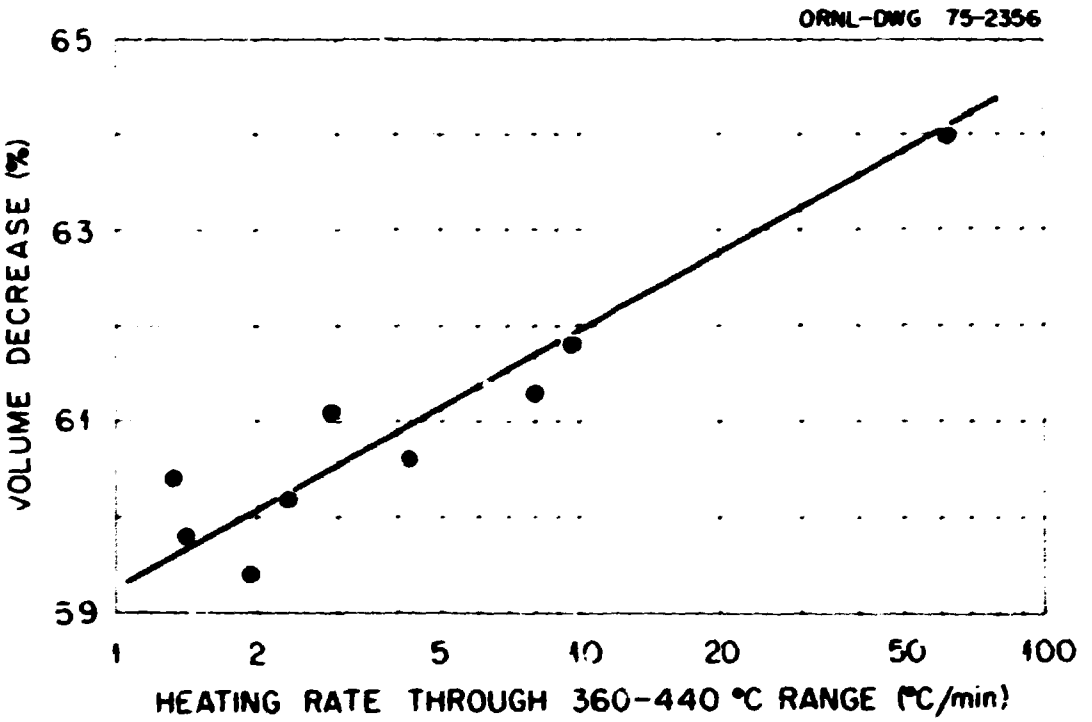

Fig. 11. Volume Decrease of Dried (110°C) Uranium-Loaded Weak-Acid (Duolite C-464) Resin During Carbonization to 1200°C as a Function of Critical Range Heating Rate.

Chemical analyses were made of the final products (Table 3). Since the uncertainty in the oxygen analyses is generally accepted to be considerably greater than that in the uranium and carbon analyses, the oxygen determination was computed by difference. The oxygen-to-uranium ratio after carbonization should be nearly equal to 2.00 (for UO_2). The oxygen determined by difference is closer to the actual value than is the analytically determined percentage.

The carbon-to-uranium ratio for Duolite C-464 shows a strongly linear correlation with the logarithm of the heating rate (Fig. 12). The linear correlation coefficient for the $y = ae^{bx}$ program was 0.9749.

Table 3. Effect of heating rate in the 360–440°C range during carbonization on composition of Amberlite weak-acid resin

Heating rate	Weight loss	Composition, %				Atomic Ratio		
		U	C	O	O[a]	C/U	O/U	O/U[a]
1.41	32.1	69.68	21.11	8.53	9.21	6.00	1.82	1.97
1.94	32.1	69.49	21.31	8.82	9.20	6.08	1.89	1.97
2.39	32.5	69.72	20.74	8.90	9.54	5.90	1.90	2.04
2.88	32.6	70.02	20.29	8.55	9.69	5.74	1.82	2.05
4.27	32.7	70.28	20.53	8.63	9.09	5.82	1.83	1.92
8.0	33.1	70.72	20.00	8.32	9.28	5.60	1.75	1.95
9.67	33.4	71.06	19.71	8.44	9.23	5.50	1.77	1.93
62.7	34.6	72.27	18.49	8.77	9.24	5.07	1.80	1.90

[a]By difference.

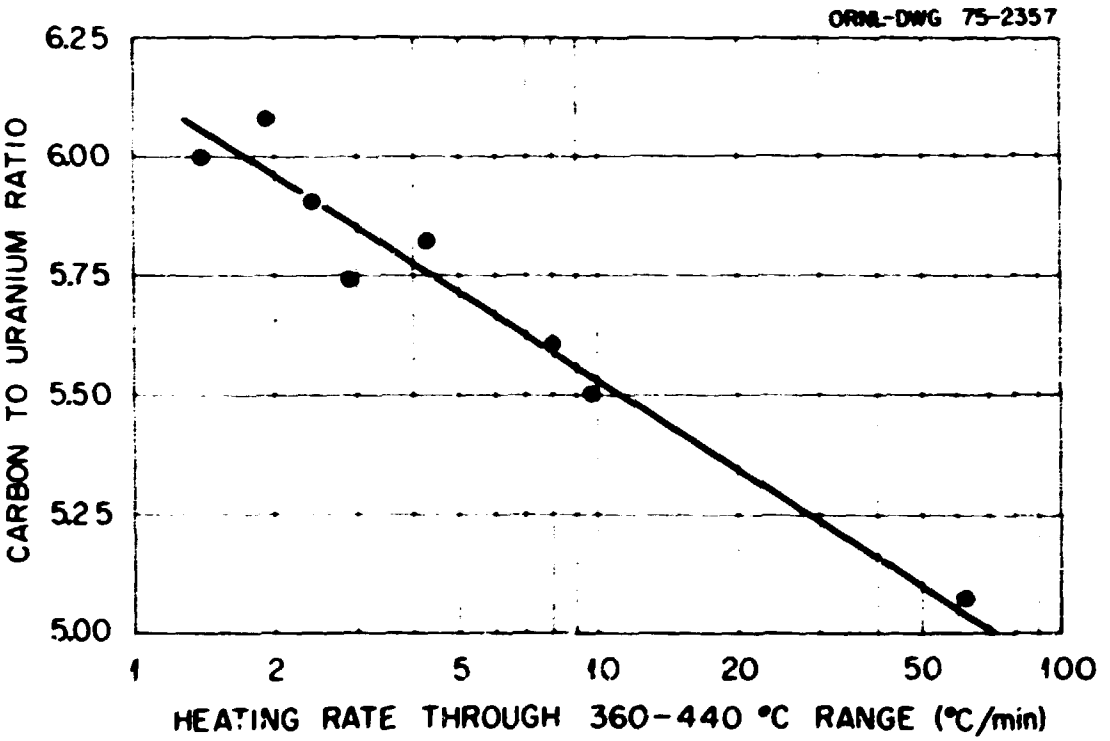

Fig. 12. Carbon-to-Uranium Ratio of Carbonized (1200°C) Uranium-Loaded Weak-Acid (Duolite C-464) Resin as a Function of Critical Range Heating Rate.

A comparison of the Duolite and Amberlite resins on the basis of carbon-to-uranium ratio (Fig. 13) is significant since comparison runs for sticking behavior clearly showed that carbon-to-uranium ratio has a strong effect on the bed agglomeration tendency at conversion temperatures. Duolite C-464 resin with higher carbon-to-uranium ratios for equivalent heating rate is thus more readily controlled during conversion than is Amberlite IRC-72. Of course both resins show reduced sintering and agglomeration at conversion temperatures with slower heating rates through the critical 360–440°C carbonization range.

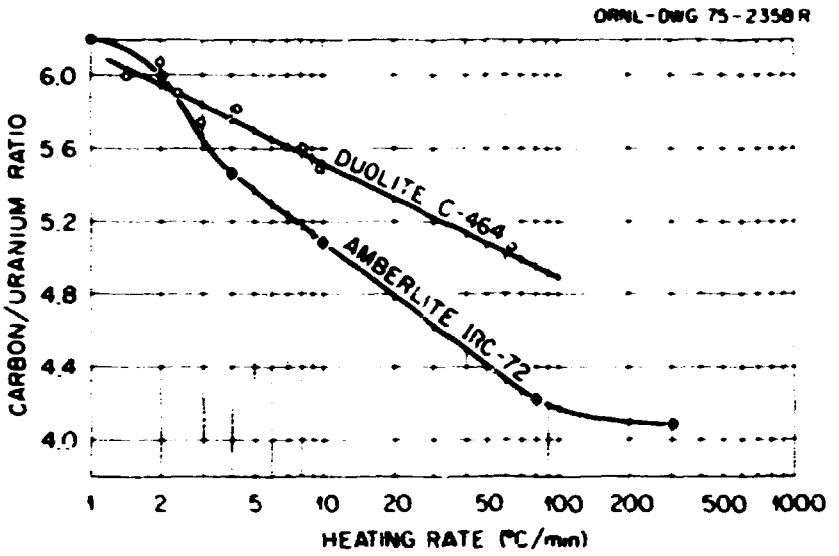

Fig. 13. Comparison of Carbon-to-Uranium Ratio of Carbonized (1200°C) Uranium-Loaded Weak-Acid Resins as a Function of Critical Range [Duolite (360–440°C), Amberlite (200–500°C)] Heating Rate.

Changes in Properties During Carbonization

The changes in weight, volume, tap density, mercury density, porosity, carbon-to-uranium ratio, and particle size with temperature during a typical carbonization run were determined by heating batches of uranium-loaded Duolite and Amberlite to sequentially increasing end points. Batches of 70 g in a 1.3 8-in. tube were heated to selected temperatures during a typical carbonization cycle and then cooled rapidly to room temperature.

The weight losses, volume losses, and tap densities for Amberlite at various processing temperatures may be compared (Fig. 14). The weight loss curve (Fig. 14) is essentially a TGA curve and describes closely the behavior shown in Fig. 6. The volume loss curve (Fig. 14) shows a similar behavior to 440°C but does not level at 500°C as does the weight loss curve. Shrinkage continues to 800°C at which point volume becomes constant to 1700°C. The tap density reflects these variations in volume and weight with a very rapid increase to 500°C, a slightly less rapid increase to 800°C, followed by a nearly constant value to conversion temperature (Fig. 14). It should be noted that this tap density divided by 0.62, the ideal packing fraction, yields an approximately true density.

The weight, volume, and tap density changes with process temperature for Duolite C-464 are shown similarly in Fig. 15. The weight loss curve follows the TGA curve in a manner similar to that observed for Amberlite. Volume loss and shrinkage continue to 900°C in an analogous manner. Some slight weight loss with concomitant shrinkage occurs to 1700°C. The gross weight and volume losses for the two resins over this temperature range are thus similar.

The change in particle size with temperature was determined by microradiography. Thirty particles were examined to determine the average particle size in microns (Fig. 16). The particle size curve parallels very closely the TGA and shrinkage curves, dropping rapidly from 515 μm at room temperature for dried particles to 375 μm at 700°C for Amberlite. The particle size remains nearly constant from 700 to 1675°C.

The variations in the carbon-to-uranium ratios as a function of temperature for the two candidate resins were similar (Fig. 17). The higher final value of the carbon-to-uranium ratio for the Duolite resin is in keeping with the results previously reported on heating rate.

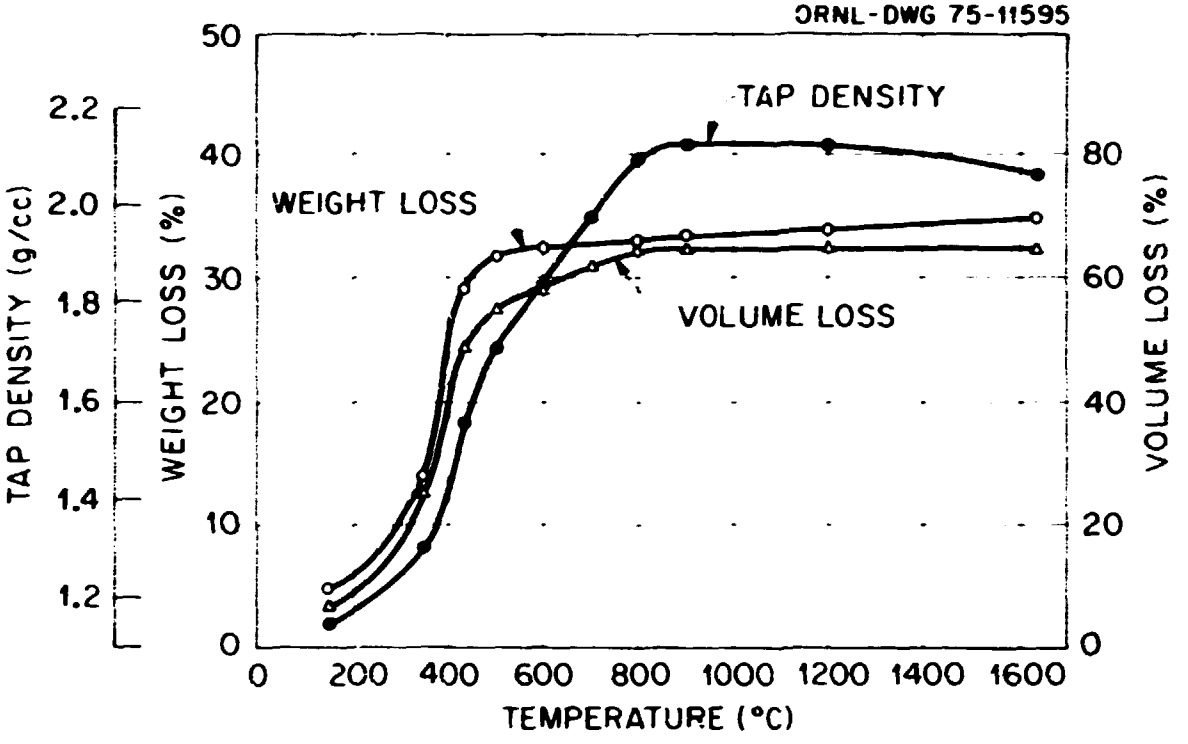

Fig. 14. Weight Loss, Volume Loss and Tap Density Variation from 150 to 1625°C for Uranium-Loaded Amberlite (IRC-72) Weak-Acid Resin.

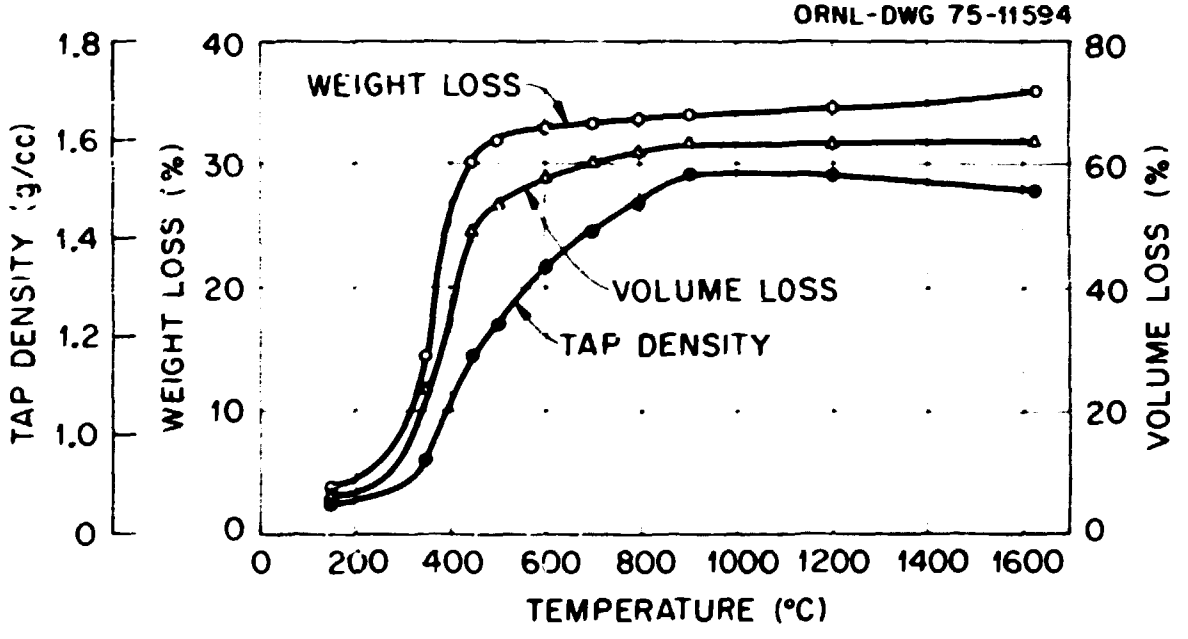

Fig. 15. Weight Loss, Volume Loss and Tap Density Variation from 150 to 1625°C for Uranium-Loaded Duolite (C-464) Weak-Acid Resin.

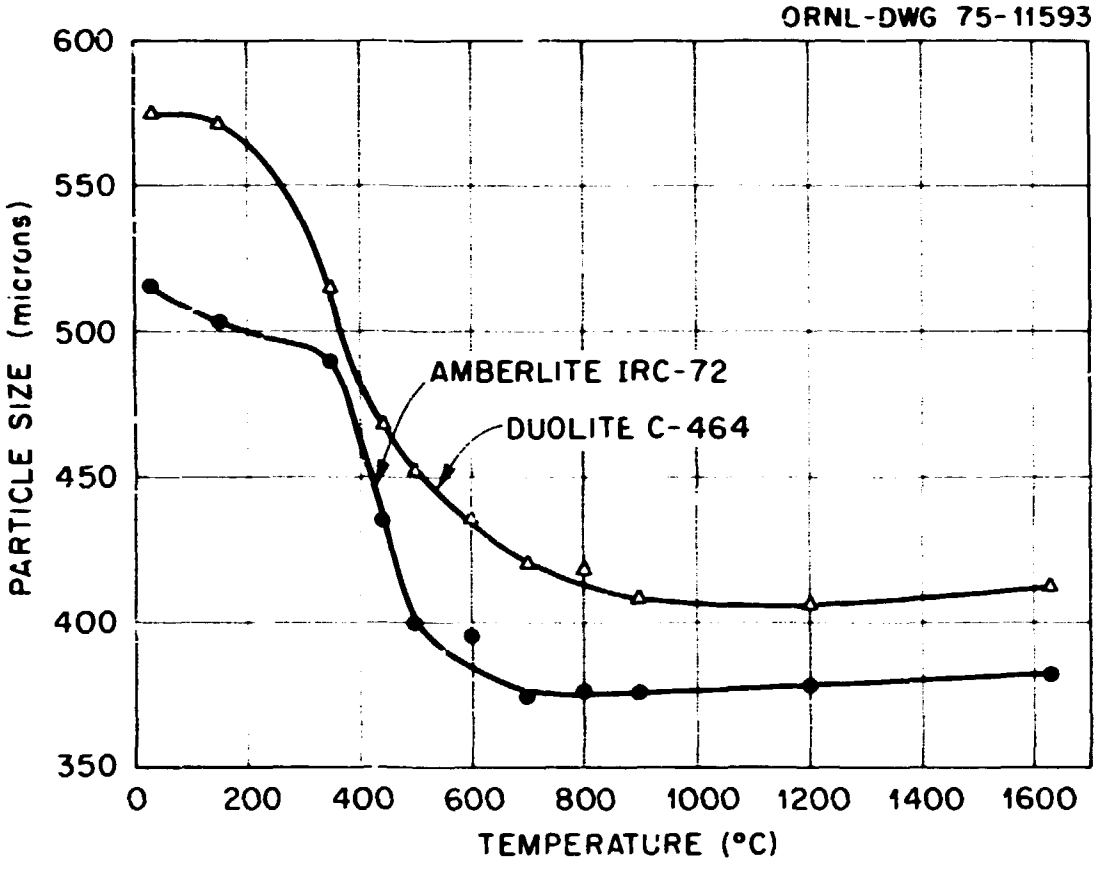

Fig. 16. Variation in Particle Size of Uranium-Loaded Duolite (C-464) and Amberlite (IRC-72) Weak-Acid Resins from 25 to 1625°C.

The mercury density was determined at 15, 75, 250, and 15,000 psi (Fig. 18). The 15,000 psi measurements for all of the Duolite material and the first three of the Amberlite were off-scale of the measuring device. The 15, 75, and 250 psi measurements were not significantly different for either type of resin. The mercury density again closely parallels the TGA behavior for both materials and is approximately 1 g/cm^3 greater than the tap density for the 15 psi measurement. When the tap density is divided by 0.62, the densities are essentially the same.

Mercury porosimetry shows that the carbonized Duolite C-464 material has a pore size of approximately 0.05 μm, which is significantly greater than the value of 0.015 μm obtained for Amberlite IRC-72 (Fig. 19). Both types of resin-derived fuel showed similar variations in pore size with process temperature from 150 to 1625°C. Pore size decreases from 150 to 440°C. From 440 to 1200°C for both materials, the pore size increases very slightly as the cumulative percent porosity increases in a fairly regular manner. The Amberlite IRC-72 shows a decrease in pore size and percent porosity as the temperature increases to 1625°C while the Duolite C-464 remains essentially unchanged. The suggested picture is one in which smaller pores are opened in increasing amounts from 150 to 440°C while destructive distillation of the resin is progressing and considerable quantities of volatiles are being liberated. From 500 to 1200°C, as this process is essentially complete, the pores apparently coalesce and enlarge. The Duolite porosity data are incomplete as the high-pressure values were not obtained due to instrument saturation.

Measurement with nitrogen of the BET surface areas at different temperatures indicated a corresponding change with process temperature (Table 4). The surface area increases rapidly from 440 to

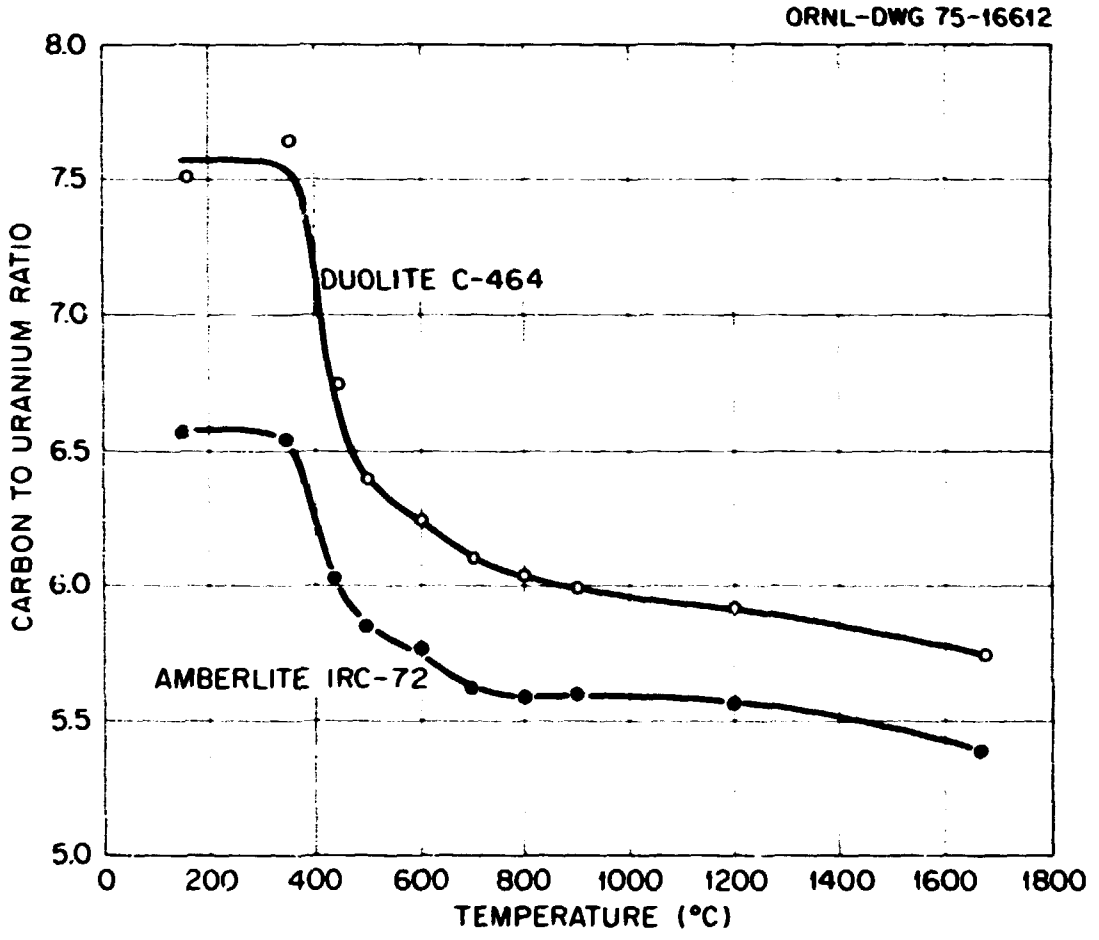

Fig. 17. Variation in Carbon to Uranium Ratio with Carbonization Temperature for Duolite (C-464) and Amberlite (IRC-72) Weak-Acid Resin-Derived Fuel Carbonized at 2°C per Min to 600°C.

1200°C with a subsequent decrease to 1625°C. Combining this information with the pore size data indicates that from 440 to 1200°C pores of virtually the same diameter increase significantly in number. From 1200 to 1625°C, the pores coalesce to some extent with a subsequent decrease in total porosity and surface area.

The development of the UO_2 phase during the carbonization process is illustrated by x-ray powder patterns (Fig. 20). Although the 500°C pattern is not shown, at this temperature the phase is just beginning to exhibit coherently diffracting regions of UO_2, and the lines are very diffuse and broad. At 700°C, the lines are still diffuse but are readily resolvable. With increasing temperature at 900 and 1200°C, the lines become increasingly sharp and well developed as the coherently diffracting regions enlarge. At 1200°C, the phase is clearly defined as widely dispersed UO_2 crystallites.

To evaluate the crystallite size of the material, a standard of well-crystallized UO_2 was ground to −325 mesh and x-rayed in a similar manner. The line intensities and width of the standard were used to correct

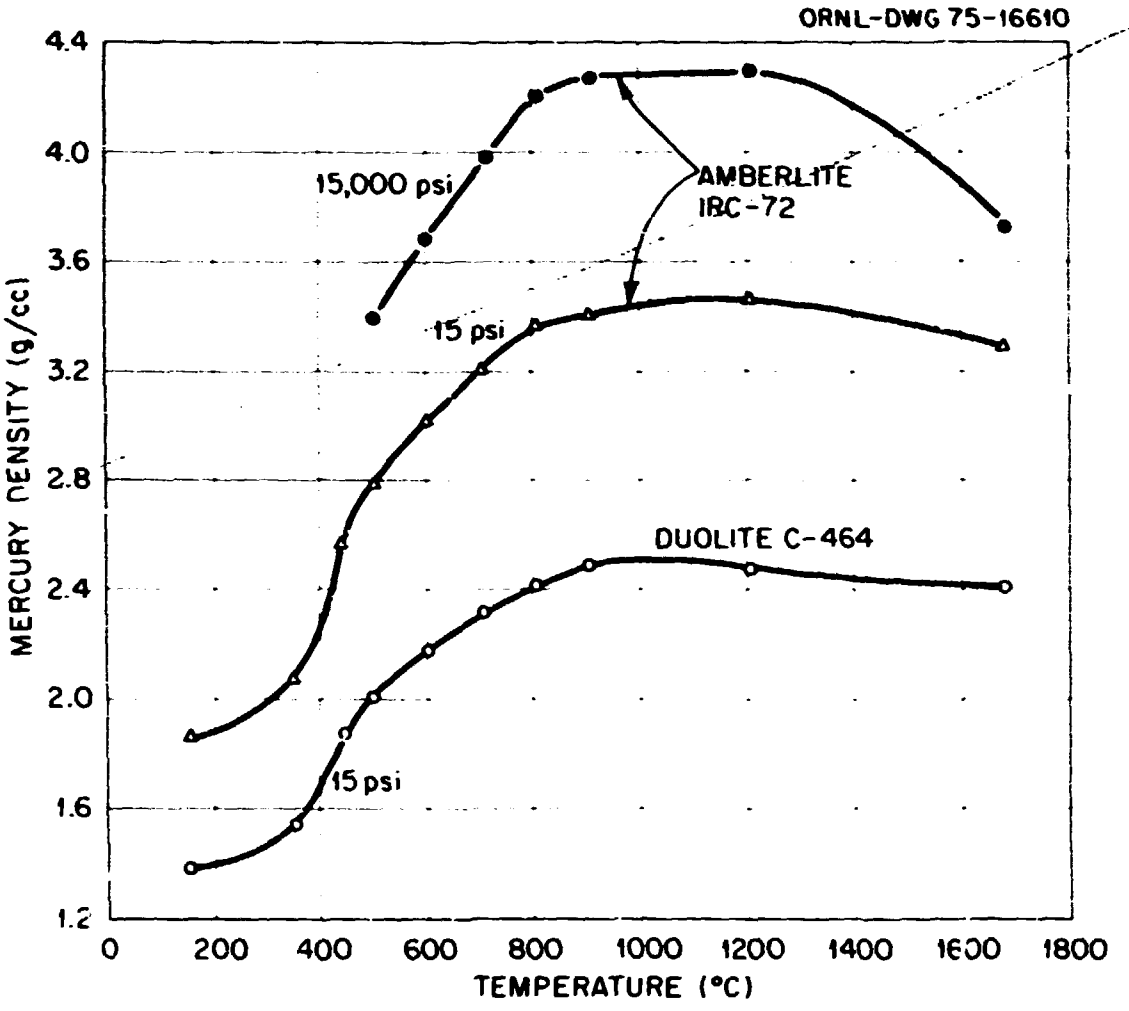

Fig. 18. Variation in Mercury Density at 15 and 15,000 psi as a Function of Carbonization Temperature for Duolite (C-464) and Amberlite (IRC-72) Weak-Acid Resin-Derived Fuel Carbonized at 2°C per Min to 600°C.

the broadening of the unknown sample. The corrected broadening was used to calculate the crystallite size for specific reflections from the Scherrer formula[14]

$$t = \frac{C\lambda}{B \cos\theta_\beta}$$

where

t = crystallite size,

C = Scherrer constant,

θ_β = angle at which maximum diffracted intensity occurs,

λ = wavelength of incident radiation, and

B = broadening = $\theta_1 \quad \theta_2$ = difference between the two extreme angles at which the intensity is 0

With a Scherrer constant of 1.0, crystallite sizes (in Angstroms) were determined (Table 5)

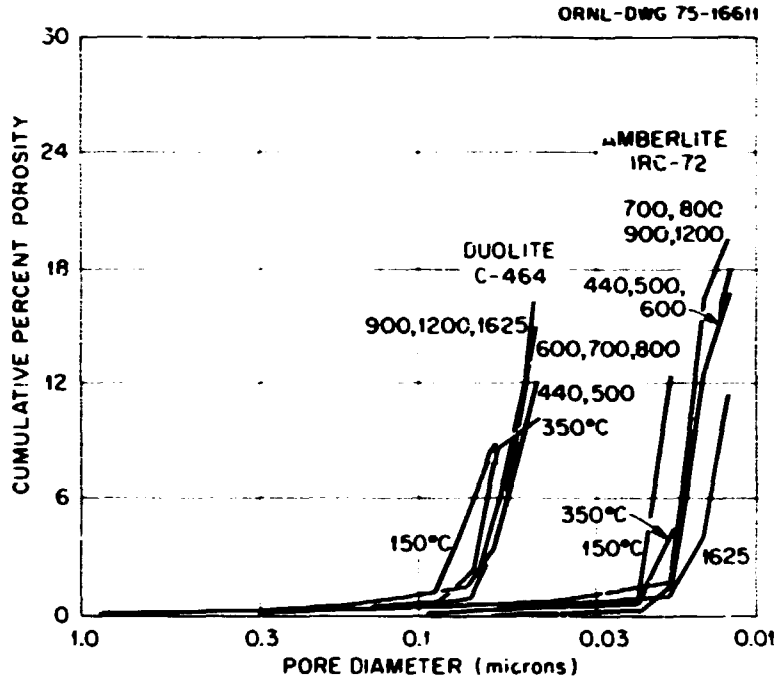

Fig. 19. Cumulative Percent Porosity Variation with Pore Diameter as a Function of Carbonization Temperature for Duolite (C-464) and Amberlite (IRC-72) Weak-Acid Resin-Derived Fuel.

Table 4. BET surface area of weak-acid resin-derived fuel as a function of process temperature

Temperature (°C)	Resin	Surface area (m^2/g)
440	Amberlite	50
1200	Amberlite	140
1625[a]	Amberlite	116
440	Duolite	91
1200	Duolite	183
1625[a]	Duolite	147

[a]To approximately 100% conversion.

The general increase in size with increasing temperature is apparent. The crystallites of UO_2 in carbonized material, even allowing for experimental uncertainty well above the anticipated ± 5 Å in the above results, are thus apparently less than 100 Å in size and finely dispersed through a porous carbon matrix.

Other Carbonization Process Parameters and Uranium Loss

Uranium lost during carbonization was collected by a gauze filter system. For a typical carbonization cycle of 2°C/min to 1200°C with 2.35 g of weak-acid resin, no counts above background were obtained on the collecting gauze or furnace parts, indicating negligible uranium loss.

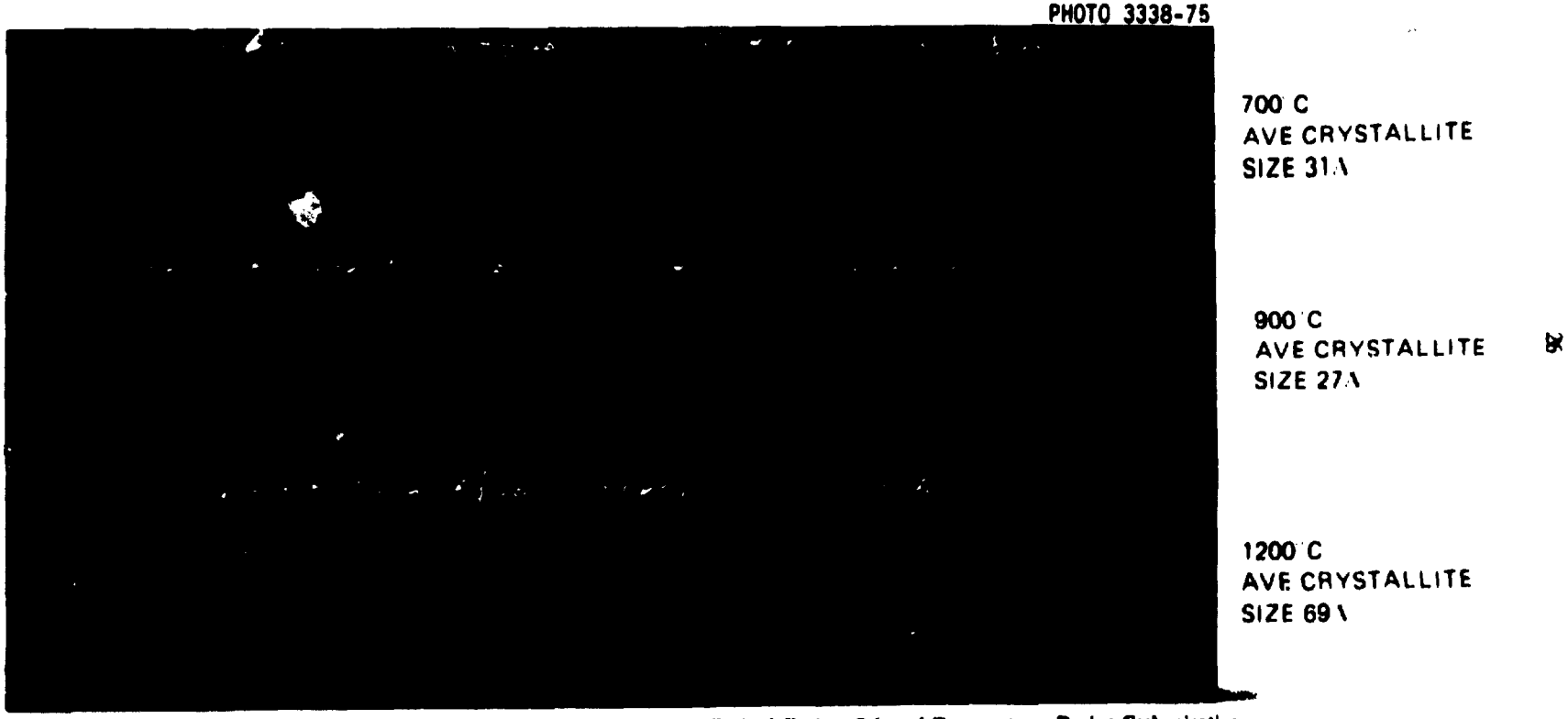

Fig. 20. X-Ray Powder Patterns of Weak-Acid Resin-Derived Fuel at Selected Temperatures During Carbonization Cycle.

Table 5. UO_2 crystallite size variation with temperature during carbonization of weak-acid resin

Sample	Temperature (°C)	Crystallite size, Å			
		(111)	(200)	(220)	Average
IE-279	500	21	26	16	21
IE-283	700	28	35	29	31
IE-285	900	25	25	31	27
IE-288	1200	71	66	70	69

A carbonization cycle on the 150-g batch at 170°C/min to 1200°C yielded the following counts (dis/min) on the furnace parts (Fig. 5):

Sight port tube	1446
Furnace lid	1368
Graphite tube adapter and insert pieces	3030

The collection gauze and the wipers used on the furnace components were ashed and analyzed for uranium. Approximately 15.3 mg of uranium was obtained which represents about 0.02% of the total uranium in the batch. Although this probably does not represent complete collection, it is indicative of the uranium loss during a very fast carbonization cycle. Hence, the slow carbonization used to maximize the carbon-to-uranium ratio is also advantageous in avoiding process loss of uranium.

Alternate carbonization media were investigated by replacing the argon fluidizing gas with air to about 270°C, the first significant TGA reaction, or with hydrogen chloride to 500°C to improve the carbon-to-uranium ratio as suggested by Bacon.[13]

When air was used, the particles were observed to change color at 270°C in a normal manner as the air was replaced by argon at that temperature. Subsequent bed behavior relating to the onset of initial smoking, and heavy smoking, indicated that air exposure had raised the temperatures of these events by 20°C. This temperature (270°C) was identified as being the maximum feasible temperature for using air as a fluidizing gas. Temperatures above 280°C produced rapid oxidation. Analyses of material in which air was substituted for argon to 270°C may be compared with data from an otherwise identical control run (Table 6). The substitution of air for argon in the initial stages of carbonization does not appear to produce a significantly different material. Although no increase in carbon-to-uranium ratio was produced, replacing with air the large volume of argon required to fluidize a batch to 250 to 270°C will save money.

Replacing argon with hydrogen chloride to 500°C raised the temperature at which the physically observable bed changes occurred by about 50 to 60°C. However, a yellowish film formed on the sight glass and furnace lid at approximately 1080 to 1100°C. This film disappeared when exposed to air. Examination with an alpha counter showed the residue to have a significant contamination level, probably of uranium. Adjustment of the heating procedure from 800 to 1200°C did not eliminate release of this material. Extensive attack on the anodized aluminum furnace parts was observed. The results of analyses on these batches (Table 7) show the advantage of increasing the carbon-to-uranium ratio by 0.5 by additions of hydrogen chloride to be far outweighed by uranium release and attack on furnace parts. The exposure behavior of the normal and air-substituted material to air was essentially identical. The hydrogen chloride-exposed material displayed considerably less apparent weight gain with time. However, this behavior was attributed to the liberation of considerable amounts of hydrogen chloride and/or uranium containing volatile species during oxidation.

Table 6. Effect of air and hydrogen chloride atmospheres on carbonization of uranium-loaded weak-acid Amberlite IRC-72 resin

Process	Carbon-to-uranium ratio	Loss (%)	
		Weight	Volume
Normal	5.57	37	67
Air substitution[a]	5.62	37	67
HCl addition[b]	6.03	38	66

[a]Air substituted for argon to 270°C.
[b]Hydrogen chloride added to argon to 500°C.

Table 7. Conversion behavior of weak-acid resin-derived fuel

Type material	Weight uranium (g)	Ar/U (l/g)	Percent conversion	1/T K ($\times 10^4$)	Tube diameter (in.)	Ar/U (l/g × 10^2 × % conversion)
A[a]	37.7	0.66	43.6	5.133	1 3/8	1.52
A	50.7	5.36	43.4	5.640	1 3/4	12.4
A	51.4	1.09	66.3	5.269	1 3/4	1.64
A	54.0	1.55	57.8	5.339	1 3/4	2.69
A	50.5	5.63	37.3	5.624	1 3/4	15.1
A	45.5	1.23	56.8	5.260	1 3/4	2.16
A	66.7	1.10	77.7	5.200	1 3/8	1.42
A	485.7	0.53	25.5	5.200	4 1/4	2.07
A	32.8	2.19	93.2	5.269	1 3/8	2.35
D[b]	50.5	0.71	46.2	5.269	1 3/4	1.54
D	152.5	0.88	41.3	5.269	1 3/4	2.14
D	150.4	1.02	45.4	5.269	1 3/4	2.24
D	56.2	1.02	63.6	5.269	1 3/4	1.60
D	55.7	1.02	68.8	5.269	1 3/4	1.49
A	272.1	0.61	50.8	5.200	4 1/4	1.19
A	41.9	1.91	39.4	5.495	1 3/4	4.85
A	87.2	0.82	39.9	5.339	2 1/2	2.07
A	117.1	0.85	27.1	5.485	2 1/2	3.15
A	154.6	0.45	45.0	5.200	2 1/2	0.99
A	154.4	0.45	43.6	5.200	2 1/2	1.03
A	107.9	1.22	35.0	5.411	1 3/4	3.48
A	28.1	2.24	47.9	5.411	1 3/4	4.69
A	107.4	2.20	53.4	5.411	1 3/4	4.12
A	29.0	1.24	35.6	5.411	1 3/4	3.49
A	108.2	1.22	35.1	5.411	1 3/4	3.47
A	28.9	1.25	29.7	5.411	1 3/4	4.21
A	56.4	4.23	31.7	5.562	1 3/4	13.35
A	57.5	4.12	44.6	5.562	1 3/4	9.23
A	57.8	3.94	43.9	5.562	1 3/4	8.97
A	57.8	2.41	53.9	5.441	1 3/4	4.47
A	57.4	2.40	39.0	5.441	1 3/4	6.15
A	57.1	2.41	39.6	5.441	1 3/4	6.08
A	120.5	0.52	48.7	5.094	1 3/4	1.07
A	57.5	5.22	47.5	5.562	1 3/4	10.98
A	57.4	7.37	72.0	5.562	1 3/4	10.24

[a]Amberlite IRC-72, Rohm and Haas.
[b]Duolite C-464, Diamond Shamrock.

Changes in Properties During Conversion

The changes in volume, weight, and conversion level at 1625 C after carbonization at 2°C/min for Amberlite IRC-72 (Fig. 21) and Duolite C-464 (Fig. 22) are similar. Weight is lost linearly with conversion due entirely to evolution of carbon monoxide. Volume shrinkage occurs somewhat more slowly than weight loss, and is not necessarily linear with conversion. The volume stability to about 25% conversion followed by a rate of shrinkage lower than the rate of weight loss produces a minimum in the tap density for both materials at approximately 50% conversion. Extended time at temperature beyond full conversion does not change the weight significantly, but does effect a small volume loss with a slight increase in tap density. The weight-loss point for the 95%-converted Duolite (Fig. 22) is anomalous in that it shows an impossible weight gain with increasing conversion level.

As expected, the variation in particle size with conversion level (Fig. 23) is similar to that seen for the volume loss. The data suggest a possible volume maximum at approximately 25% conversion. However, this result is difficult to rationalize so further work on this is needed to better define the precise manner in which particle diameter and volume change with conversion.

The mercury density variation with conversion level was measured (Fig. 24) except for the 15,000 psi values for Duolite C-464 which were not obtained as the values were off-scale on the measuring device. The

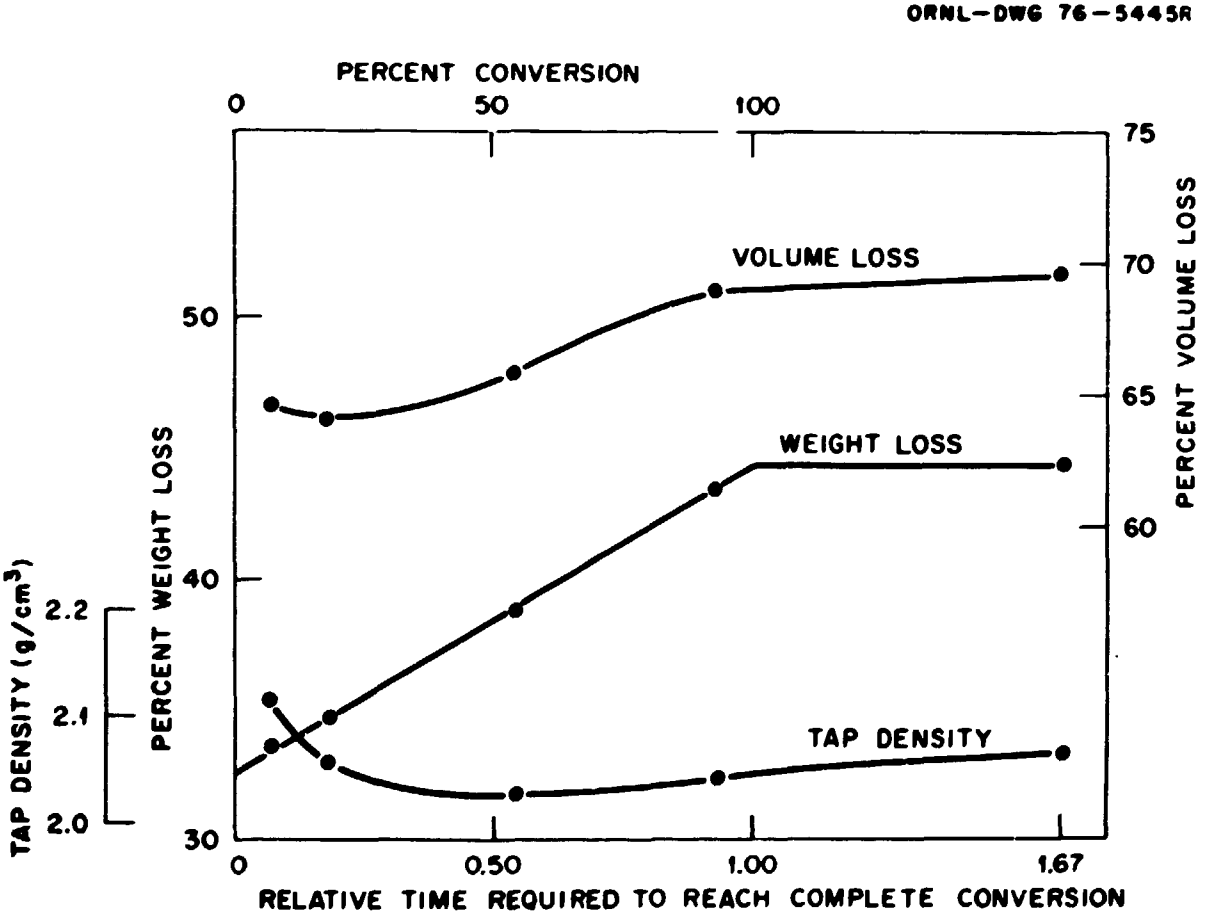

Fig. 21. Weight Loss, Volume Loss and Tap Density Variation as a Function of Conversion Level at 1625°C for Uranium-Loaded Amberlite (IRC-72) Weak-Acid Resin.

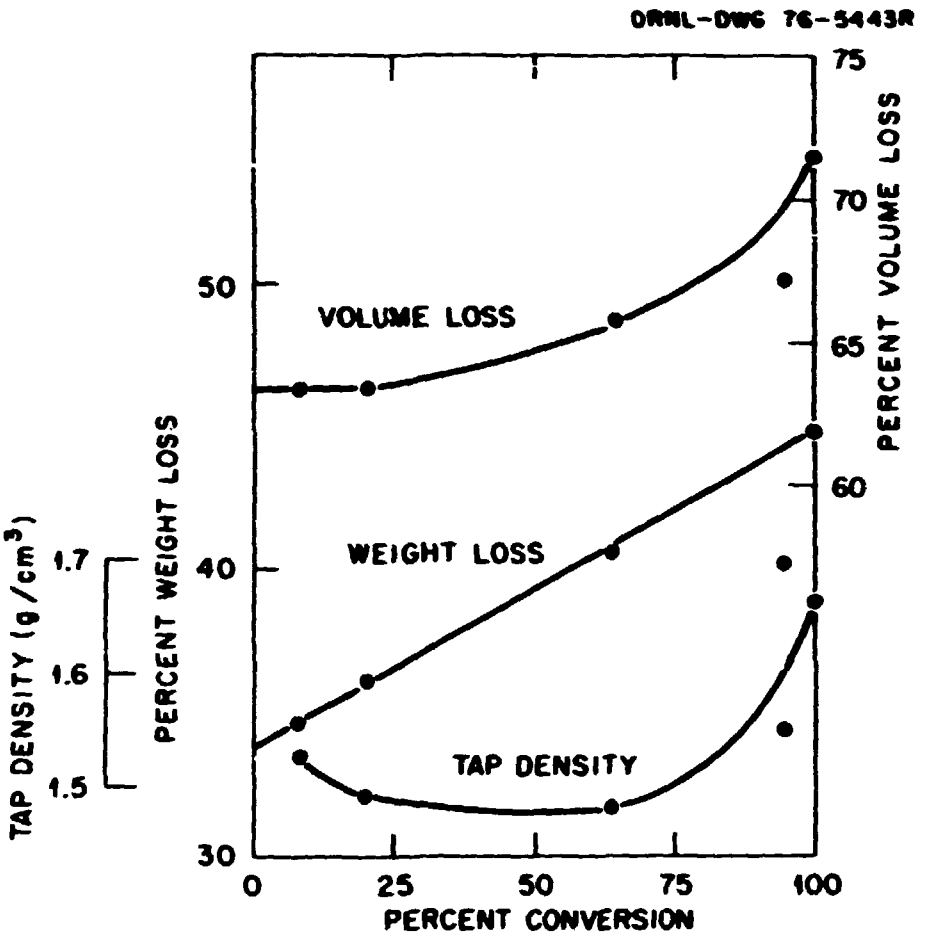

Fig. 22. Weight Loss, Volume Loss and Tap Density Variation as a Function of Conversion Level at 1625°C for Uranium-Loaded Duolite (C-464) Weak-Acid Resin.

15, 75, and 250 psi values were not significantly different and are shown as a single value. The variation closely follows that observed for the tap density with a minimum at approximately 25 to 30% conversion. The 15,000 psi Amberlite curve is not conclusive due to the small number of points but does show a similar tendency. The values for the tap density divided by 0.62, the ideal packing fraction, are essentially identical to those obtained by 15, 75, and 250 psi mercury.

The pore size distribution in nominally 35%-converted material as determined by mercury porosimetry (Fig. 25) shows the Duolite resin to have a wide range of pore sizes with the majority lying between 0.10 and 0.015 μm with an equal distribution between 0.05 and 0.025 μm. The Amberlite has a much more restricted pore size with virtually all pores smaller than 0.16 μm. Both resins approach an ultimate apparent density (to 15,000 psi mercury) of approximately 3.9 g/cm^3 for the carbonization conditions employed in this study.

Conversion Rate and Thermodynamics

The extent of conversion of weak-acid-resin derived fuel was found to be controlled by the temperature and specific gas flow. The specific gas flow is calculated as liters of argon per gram of uranium normalized to per cent conversion obtained. The conversion behavior of different sized batches at different

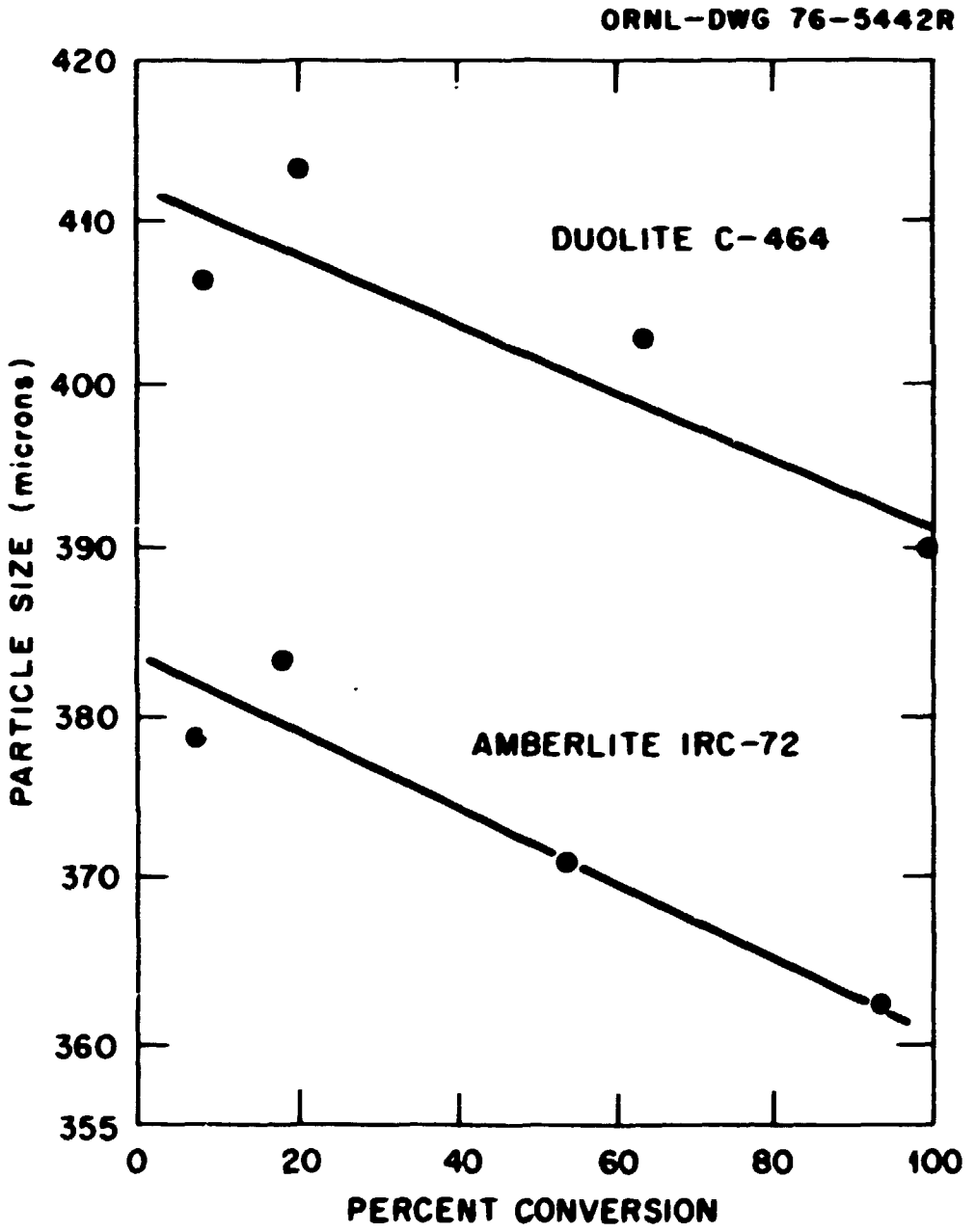

Fig. 23. Variation in Particle Size with Conversion Level of Uranium-Loaded Duolite (C-464) and Amberlite (IRC-72) Weak-Acid Resins at 1625°C.

temperatures and gas flows is shown in Table 7. The variation with temperature is shown in Figure 26 with a regression line fit for $y = ax^b$ with a correlation coefficient of 0.945 shown as a dashed line. The pertinent reaction curve predicted from thermodynamics is shown as a solid line. Duolite and Amberlite resins were not significantly different.

These results indicated that conversion is occurring to a somewhat greater extent than is predicted from classical bulk thermodynamics.[7] This behavior could be attributed to $2\gamma/r$ contributions from the small

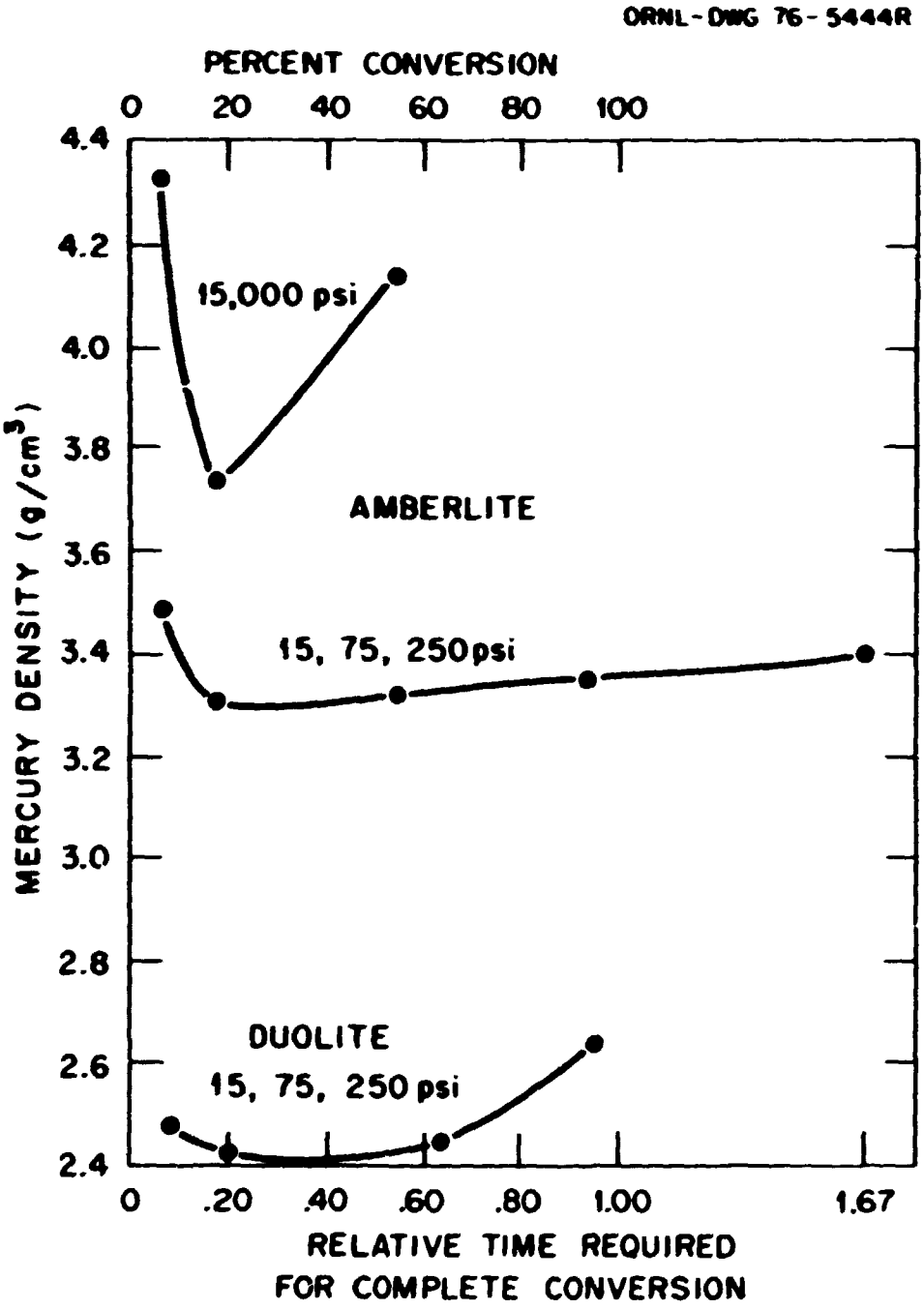

Fig. 24. Variation in Mercury Density as a Function of Conversion Level at 1625°C for Uranium-Loaded Duolite (C-464) and Amberlite (IRC-72).

curvature radius of the pores, where γ is the surface free energy and r the radius of curvature; other contributions could be due to temperature measuring error or to a second reaction occurring at a significantly greater rate at higher temperatures.

Parallel temperature measurements carried out with a platinum vs Pt 10% Rh thermocouple in the bed differed from an optical pyrometer reading on the outside tube wall opposite the thermocouple by

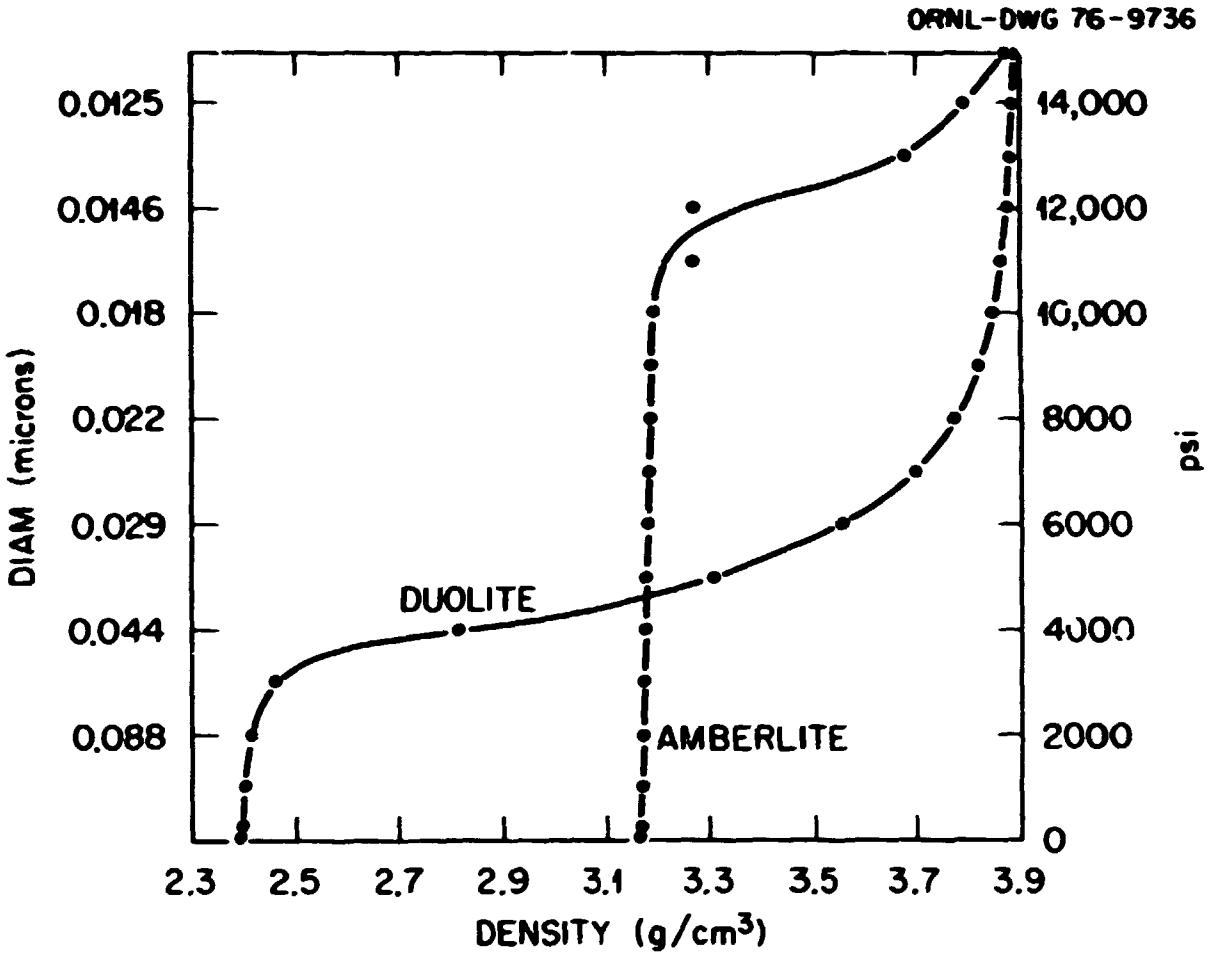

Fig. 25. Pore Size Distribution Determined by Mercury Porosimetry in Duolite C-464 and Amberlite IRC-72 Partially Converted Weak-Acid Resin.

+19.1°C, and by −6.9°C relative to an optical reading of 1450°C at the control sight port on the tube wall. The temperature divergence between the experimental data and the thermodynamic values of 8° at 1525°C and 54° at 1665°C (Fig. 26) can be attributed therefore, in part, to the error in measuring true effective bed temperature with an optical pyrometer on the exterior tube wall.

Our recent data indicate that conversion of up to 7% is occurring at 1200°C, considerably below the predicted reaction region. This behavior, possibly due to the $2\gamma/r$ contribution to the free energy from the small (~ 0.015 to 0.05 μm diam) porosity in the kernels, is apparently less important since pores may be sealed off rapidly at 1200°C once this level of conversion is obtained. This factor may be significant in the apparent conversion rate discrepancy.

A second conversion reaction may increase to enlarge the divergence of the predicted and experimental values. As will be shown later, conversion of UO_2 to $UC_{1-x}O_x$ proceeds at increasing rates relative to the $UO_2 \rightarrow UC_2$ reaction as the temperature goes up.

The effect of fluidizing condition on the effective bed temperature and the measured bed temperature is significant in controlling conversion levels obtained for different runs or in different equipment. Parallel bed thermocouple and optical wall temperature measurements for various fluidizing conditions (Fig. 27)

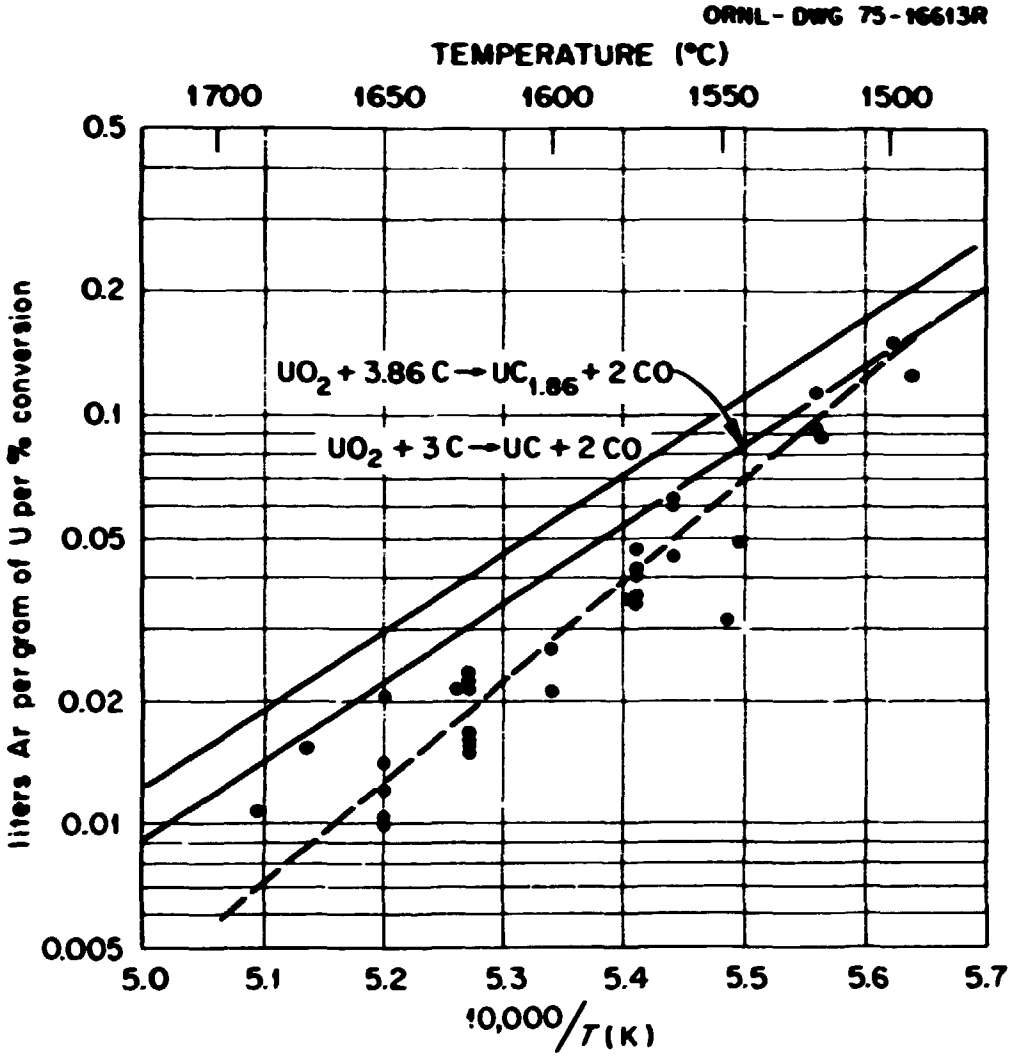

Fig. 26. Conversion Behavior of Weak-Acid Resin-Derived Fuel.

show that as flow is decreased from 8.0 to 7.0 and 6.0 liters/min, the temperature rises correspondingly if the bed is free flowing. An increase to 10.1 liters/min produces a corresponding temperature drop. However, bed temperature behaves erratically in relation to both gas flow and the control measurement if particle sticking or agglomeration occurs and the bed is no longer free flowing. Considerable variation in the conversion level could be obtained with a specific temperature and gas flow if bed fluidization behavior is not closely monitored.

Batch size and particle size have only a small, if any, effect on the conversion level under these conditions (Table 8). On the other hand, specific gas flow rate has a large effect.

The strong dependence of percent conversion on gas flow (Fig. 26) is in accordance with the model described by Lindemer[1,2] and Beatty[5] in which an increase in argon flow rate would be expected to increase the reaction rate. If sufficient porosity is available so that diffusion is not the rate limiting step in the carbon monoxide removal, the percent conversion can be predicted by using published values for the equilibrium partial pressure of carbon monoxide for the appropriate conversion reaction. However, Johnson et al.[8] found that increasing the gas flow during the conversion process from 1 scfm to 3 scfm actually

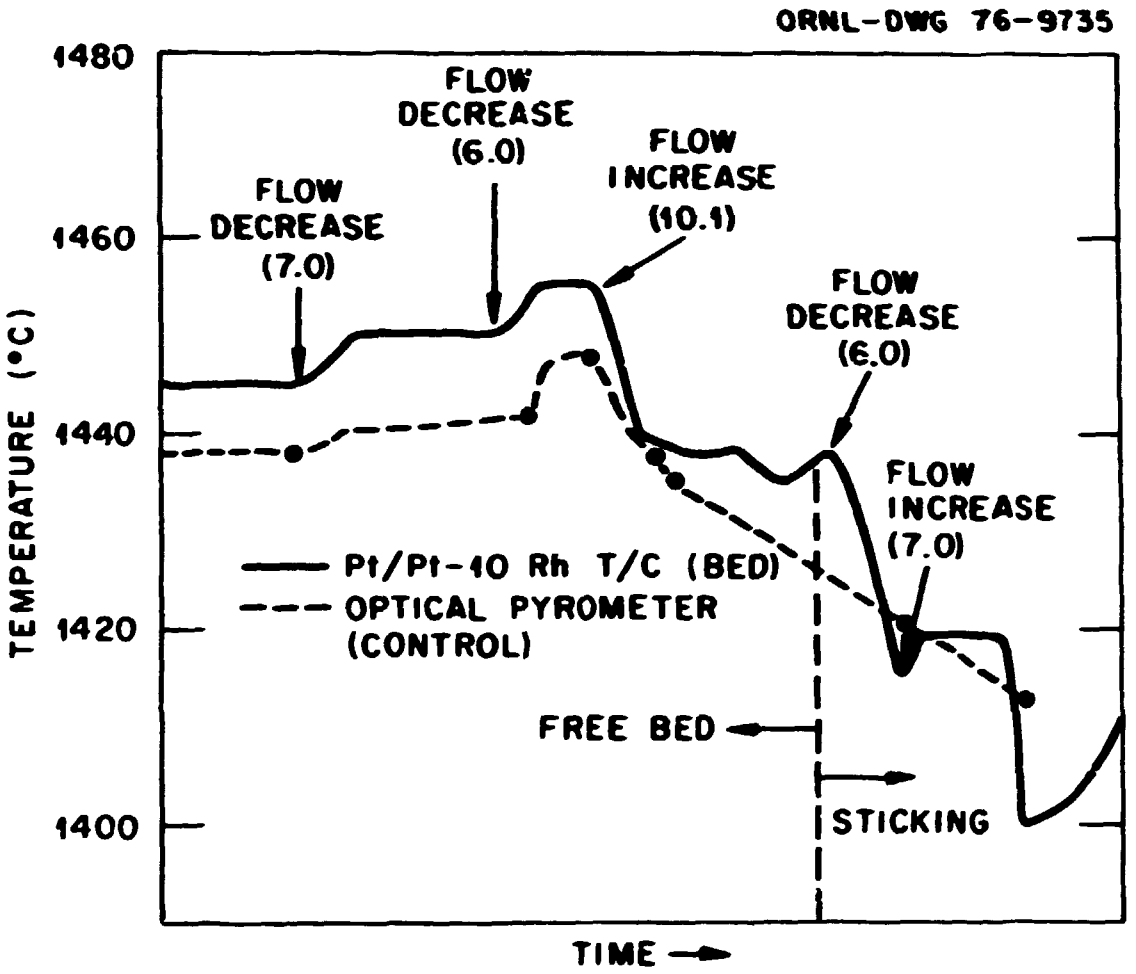

Fig. 27. Temperature Variation in a Fluidized Bed as a Function of Bed Behavior and Fluidizing Gas.

Table 8. Conversion behavior of weak-acid resin-derived fuel

Particle size[a]		Batch size[a] (g)	Total gas flow (l/g U)	Conversion level (%)
(mesh)	Diameter (μm)			
25–30	590–710	40	1.17	29.7
35–40	420–500	40	1.17	35.6
25–30	590–710	150	1.17	35.1
35–40	420–500	150	1.17	35.0
35–40	420–500	40	2.1	47.9
35–40	420–500	150	2.1	53.4

[a]Dried, loaded IRC-72.

decreased the conversion level. This was attributed to a decrease in particle temperature as the gas flow was increased and more heat moved from the particles to the argon. It was also argued that this decrease in particle temperature would not be detectable on the exterior of the reaction chamber. Using Lindemer's model, Johnson, et al.[8] calculated a decrease of 100°C in the effective particle temperature without a corresponding decrease in the measured wall temperature. An increase in the gas flow does produce a decrease in bed temperature (Fig. 27). However, the observation of this decrease is rapidly and uniformly followed by the control pyrometer observation through the outside of the fluidizing tube as long as the bed remains fluidized. When the bed begins to agglomerate, and fluidization conditions are uncertain, this correspondence is lost and the effect may be reversed to where a higher flow may yield a higher temperature, in accordance with the behavior observed by Johnson et al.[8] Johnson's experiments used a constant fluidizing gas flow from room temperature to 1800°C, whereas the experiments in this study used a decreasing gas flow as temperature was increased. Pilloton states that the minimum fluidization gas flow is proportional to the reciprocal of the kinematic viscosity of the fluidizing gas.[15] Although gas viscosities at high temperatures are not readily available, Nestor has derived an expression for their temperature dependence.[16] From these relationships Pilloton has shown that the temperature coefficient of the minimum gas mass flow for fluidization shows a decrease of a factor of 25/1 from 25°C to 1800°C.

It is thus conceivable that the conditions observed by Johnson et al.[8] with a constant fluidizing gas flow may have led to inadequate fluidizing conditions during carbonization for the lower gas flow employed. This may have resulted in the carbonized resin having different properties before and during conversion, therefore the resin's behavior during the conversion process would have been unpredictable.

Product Phase Evaluation

Studies to determine the phase content of converted material were done by varying the conversion temperature and conversion atmosphere. The relative amount of the $UC_{1-x}O_x$ phase, as determined semiquantitatively from x-ray powder camera films (Fig. 28) are shown in order of decreasing amount of $UC_{1-x}O_x$ (Table 9).

The run with argon + 0.75 equilibrium p_{CO} had no detectable $UC_{1-x}O_x$ phase and showed only UO_2 and UC_2. No other phases were observed. The runs at 1505°C and at 1625°C with 4% H_2 addition had essentially the same content of $UC_{1-x}O_x$ with the balance UO_2 and UC_2. The $UC_{1-x}O_x$ was in all instances a minor phase.

It appears that lower temperatures with corresponding longer times result in less of the $UC_{1-x}O_x$ phase being present in the kernels. Also, the use of 0.75 equilibrium p_{CO} to increase the time at a given temperature for an equivalent conversion level by a factor of 4 essentially eliminates the $UC_{1-x}O_x$ phase from the converted kernels. The use of a 4% H_2 addition decreases the amount of $UC_{1-x}O_x$ approximately as much as does lowering the conversion temperature by 120°C. The exposure of the carbonized resin to air before conversion does not appreciably affect the amount of this phase. As the 66% converted argon run is comparable to conditions normally used in fuel fabrication, partially converted weak-acid resin fuels nominally contain UO_2, UC_2, and minor amounts of $UC_{1-x}O_x$.

The decreasing amounts of $UC_{1-x}O_x$ as temperature is decreased indicates that the $UO_2 \rightarrow UC_{1-x}O_x$ reaction is more favorable kinetically as temperature is increased relative to the $UO_2 \rightarrow UC_2$ conversion. Assuming that a $UC_{1-x}O_x \rightarrow UC_2$ reaction exists, it must be slower than the $UO_2 \rightarrow UC_2$ reaction as longer times show decreased levels of $UC_{1-x}O_x$. Retarding conversion by addition of carbon monoxide allows a closer approach to equilibrium for the solid state reactions. The addition of hydrogen probably provides a more efficient transport mechanism for the $UC_{1-x}O_x \rightarrow UC_2$ reaction.[12]

A wide range of final kernel compositions and densities can be fabricated depending upon the specific carbonization rate and the percent conversion (Table 10).

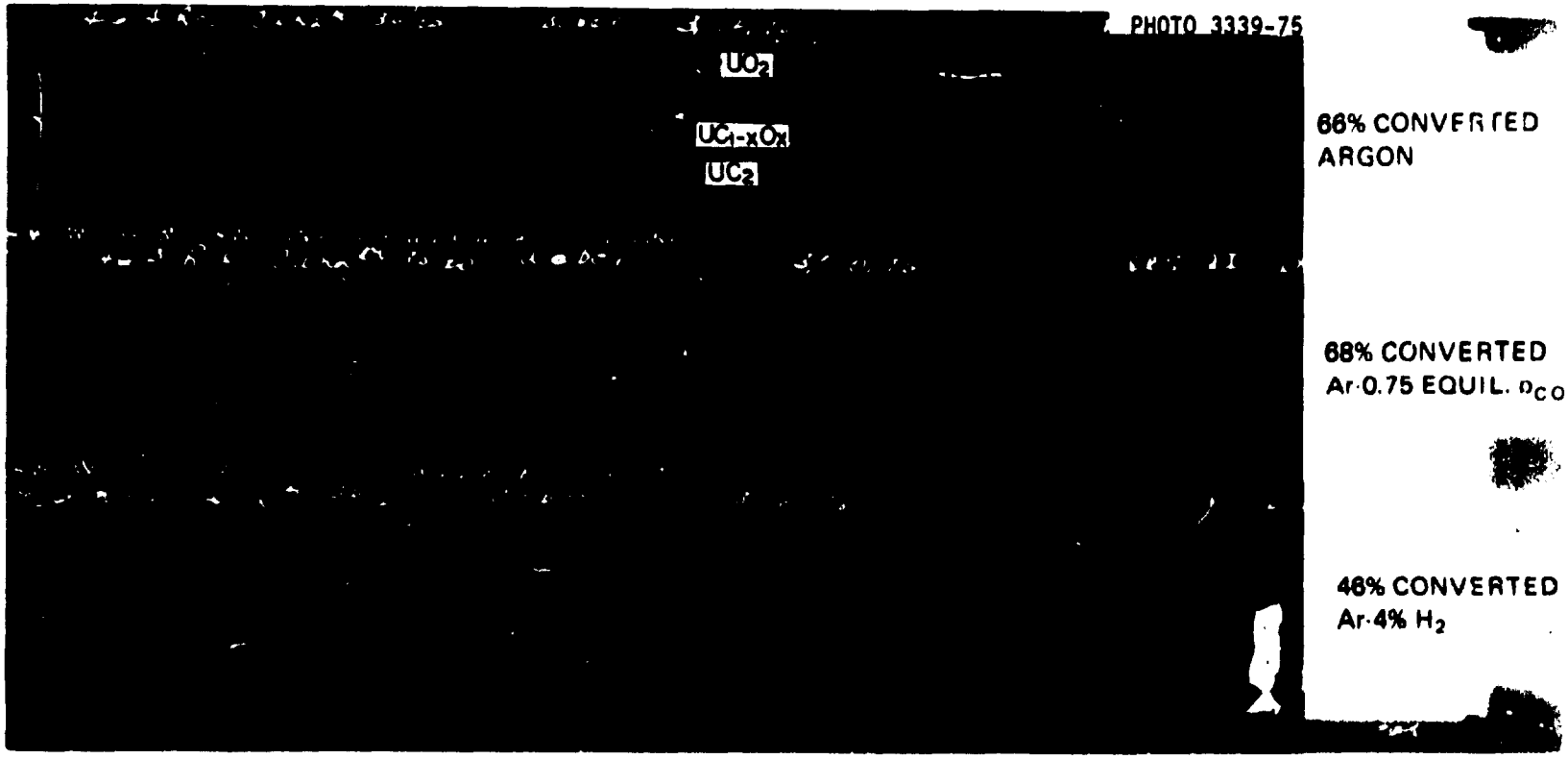

Fig. 28. X-Ray Powder Patterns of Partially Converted (1625°C) Weak-Acid Resin-Derived Fuels.

Table 9. Variation in $UC_{1-x}O_x$ content with different conversion conditions in partially converted weak-acid-resin fuel

Temperature (°C)	Conversion conditions	Conversion (%)	Relative amount
1625	Argon	66	Medium
1628	Argon exposed to air before conversion	57	Medium
1625	Argon–4% H_2	46	Weak
1505	Argon	37	Weak
1628	Argon + 0.75 equilibrium p_{CO}[a]	68	Absent

[a]Fourfold increase in time required to complete equivalent conversion.

Table 10. Kernel forms prepared from weak-acid resin for irradiation testing

Kernel composition[e]	Conversion (%)	Carbonization rate (°C/min, 200–500°C)	Kernel density (g/cm^3)	Irradiation test
$U{\cdot}C_{5.5}{\cdot}O_{2.0}$[a]	0	2	3.22	OF-2[b]
$U{\cdot}C_{4.6}{\cdot}O_{2.0}$[a]	0	40	3.66	HRB-9,[c] -10 OF-2
$U{\cdot}C_{5.5}{\cdot}O_{1.7}$[a]	15	2	3.12	OF-2
$U{\cdot}C_{4.4}{\cdot}O_{1.7}$[a]	15	6	3.17	HRB-7, -8, 9, 10
$U{\cdot}C_{5.1}{\cdot}O_{1.5}$[a]	25	2	3.17	OF-2
$U{\cdot}C_{4.6}{\cdot}O_{1.0}$[a]	50	2	3.11	HRB-9, -10, OF-2
$U{\cdot}C_{4.1}{\cdot}O_{0.5}$[a]	75	2	3.03	HRB-9, -10, OF-2
$U{\cdot}C_{3.7}$[d]	100	2	3.01	HRB-9, -10, OF-2
$U{\cdot}C_{2.6}$[d]	100	6	5.28	HRB-7, -8, -9, -10, OF-2
$U{\cdot}C_{5.3}{\cdot}O_{1.7}$[d]	15	2	2.41	HRB-11
$U{\cdot}C_{4.8}{\cdot}O_{1.0}$[d]	50	2	2.45	HRB-11
$U{\cdot}C_{4.5}{\cdot}O_{0.6}$[d]	70	2	2.53	HRB-11
$U{\cdot}C_{5.2}{\cdot}O_{1.4}$[d]	30	2	2.42	HRB-11

[a]Amberlite IRC-72.
[b]OF—Oak Ridge Research Reactor in flux trap (core) facility.
[c]HRB—High Flux Isotope Reactor Test in removable beryllium region.
[d]Duolite C-464.
[e]The compositional notation does not imply the existence of compounds with these specific molar ratios but only with this ratio of moles in the chemical analysis of the final product.

Uranium Loss During Conversion

Uranium loss during conversion was determined by use of a water-cooled furnace probe to be 38 mg for 150 g of WAR (68 g U) shape separated rejected kernels 73% converted at 1650 to 1800°C. Alpha counting of the probe yielded 348 dis/min. After a 98% conversion at 1775°C of a 150-g batch of spherical particles, alpha counting of the probe showed 787 dis/min. Again the particles impinged directly on the probe. As these two runs represented combinations of worst-case situations including rejected particle shapes, direct particle impingement, and full conversion at high temperatures, the values of uranium loss during normal conversion conditions are anticipated to be somewhat less than 0.035%.

Fluidization Control During Conversion

The agglomeration tendency of the microspheres at high temperature is sensitive to the amount of excess carbon contained (Figs. 8, 12, and 13) as a function of carbonization rate. The density of fully reduced particles varies from <3.0 g/cm^3 for two excess moles of C:UC_2 to 5.28 g/cm^3 for one mole of excess C:UC_2 (Table 10). Fully reduced materials of lower C:U have not been prepared, but densities above 6.0 g/cm^3 would be expected. As indicated earlier, nonagglomerating microspheres with C:U ≈ 6 as carbonized can be fully reduced with excellent control. However, two operational difficulties are encountered in reducing particles having a C:U much below 6 as carbonized: the open porosity is reduced so that the reduction rate plots (Fig. 4) do not apply, and the particles agglomerate so that such a partially reduced batch cannot be assured to have equal particle-to-particle conversion.

A study was done to establish a *sticking parameter* which could be used for different batch sizes, tube sizes, cone angles, cone designs, and frits. The problem arises in the different sticking behavior observed for the same size batch in different tube sizes and cone angles for different density particles, or for different size batches in the same tube. Normalizing the gas flux with tube area yields only a partial solution. As the agglomerating tendency is resisted by the kinetic energy of the particles, a time-averaged minimum mean particle kinetic energy might well be a useful parameter. However, this value is difficult to evaluate for different bed configurations and fluidizing conditions for all positions in the bed.

Comparative agglomeration or *sticking* during conversion of weak-acid resin-derived fuel was measured with an injector pressure gage. The conversion time during which different agglomeration behavior was observed is a function of gas flux with respect to particle surface area (Fig. 29). Sticking behavior is strongly gas-flow dependent. A conversion level of 50% is free from sticking at the highest gas flow, while any conversion level in excess of 15% exhibits some sticking behavior at the lowest gas flow studied. Additionally, in all of the runs studied, sticking appeared to follow a regular pattern of gradually deteriorating bed fluidization with time at conversion temperature.

Batches which have agglomerated are often refluidized by lowering the temperature approximately 100°C and then returning to conversion temperature. Also, decreasing the conversion temperature makes it possible to complete conversion runs under conditions which would otherwise yield unacceptable agglomeration. Similarly, sticking behavior is strongly temperature dependent.[17]

In another approach used to avoid the bed agglomeration problem, a porous buffer coating can be applied to the particles after carbonization. This allows the bed to be fluidized at 1800°C for any length of time without sticking, while allowing carbon monoxide to be removed rapidly through the buffer. Further, application of the buffer immediately following carbonization fixes the volume inside the coating at the volume of the kernel. The buffer does not change dimensions significantly while the fuel is being converted to carbide. In some experiments this resulted in a void between the kernel and buffer, while in other experiments the buffer prevented shrinkage of the kernel during reduction. In either case the free volume

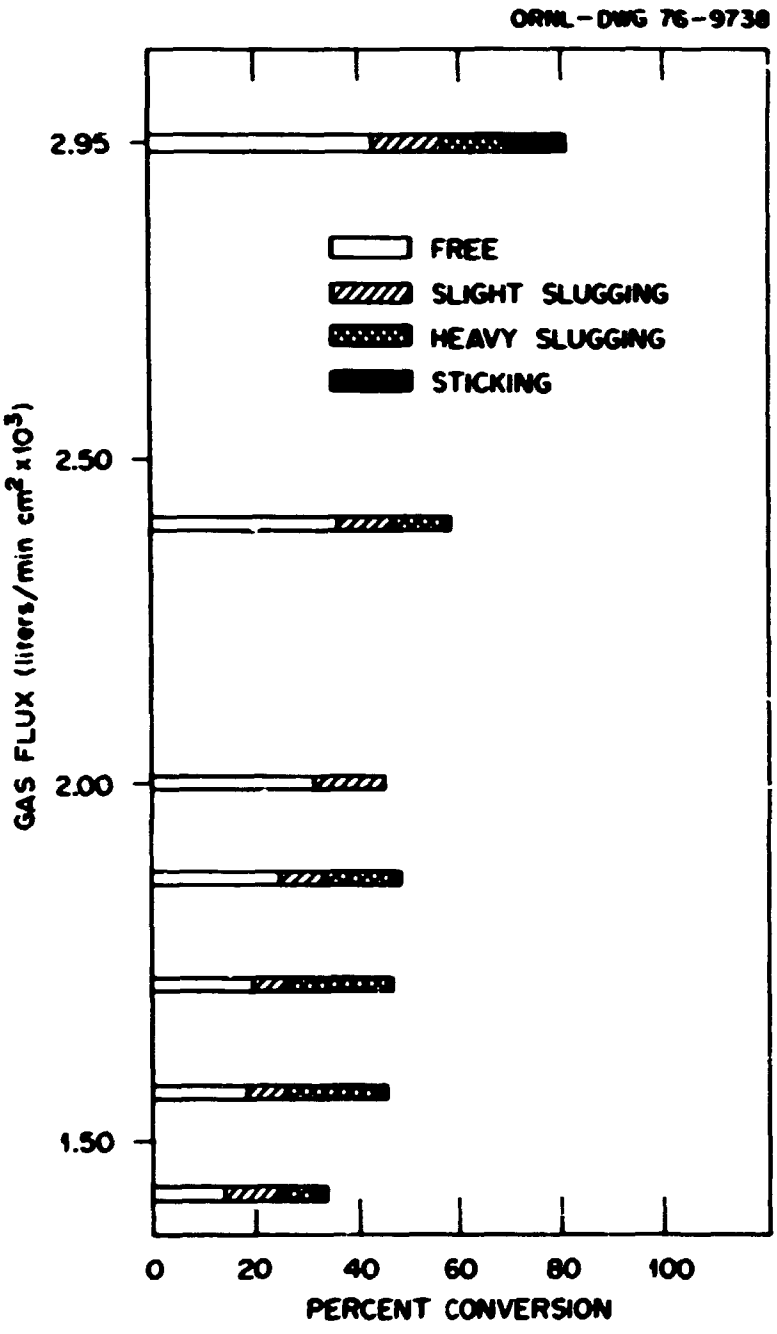

Fig. 29. Sticking Behavior of Weak-Acid Resin-Derived Fuel During Conversion as a Function of Gas Flux.

associated with the kernel, exclusive of the buffer, is a direct function of kernel volume. This should be advantageous in particle design where a range of kernel diameters and buffer thicknesses must be accommodated. When kernel shrinkage is prevented, carbothermic reduction of the fuel can be completed in about 10 min at 1800°C.

Reactivity with Air

One-gram batches of resin carbonized to 600 or 1200°C and converted at 1600°C were exposed to room atmosphere to determine the reactivity with air. After 75 hr, the weight increases of the particles treated at 600, 1200, and 1600°C were about 6, 2, and 1% respectively. Effects of exposure rate on final weight gain were insignificant though weight gains during the first hour were about twice as great in the open beakers as in the uncapped bottles. During the first 10 min, the particles carbonized to 600°C increased in weight nearly 3% in the bottles and nearly 5% in the beakers. Weights of all batches increased uniformly through a 27-hr measurement, then fluctuated over a small range with no apparent pattern. This may have been due to variations in room humidity; but humidity was not monitored in this experiment. None of the microspheres examined showed any signs of disintegration, even after weight gains as high as 6%. Even the most reactive particles, those heated to only 600°C, remained intact and did not burn when exposed to room atmosphere for long times. The particles carbonized at either 600°C or at 1200°C were exposed to air for five days, then reheated to 1200°C. The microspheres originally heated to only 600°C partially disintegrated when reheated, while those originally treated at 1200°C remained intact and returned to approximately their original weight when reheated. This suggests that uranium-loaded WAR treated at 1200°C or higher temperature may be handled in air if necessary, but there is one restriction: The particles do initially react rapidly enough to produce noticeable heat. In small batches, they simply get warm but do not burn; in large batches it would be necessary to cool the material to avoid a fire hazard.

Materials carbonized through the critical heating rate range, fully carbonized, and fully reduced to dicarbide clearly became less reactive with the room atmosphere with further thermal treatment (Fig. 30).

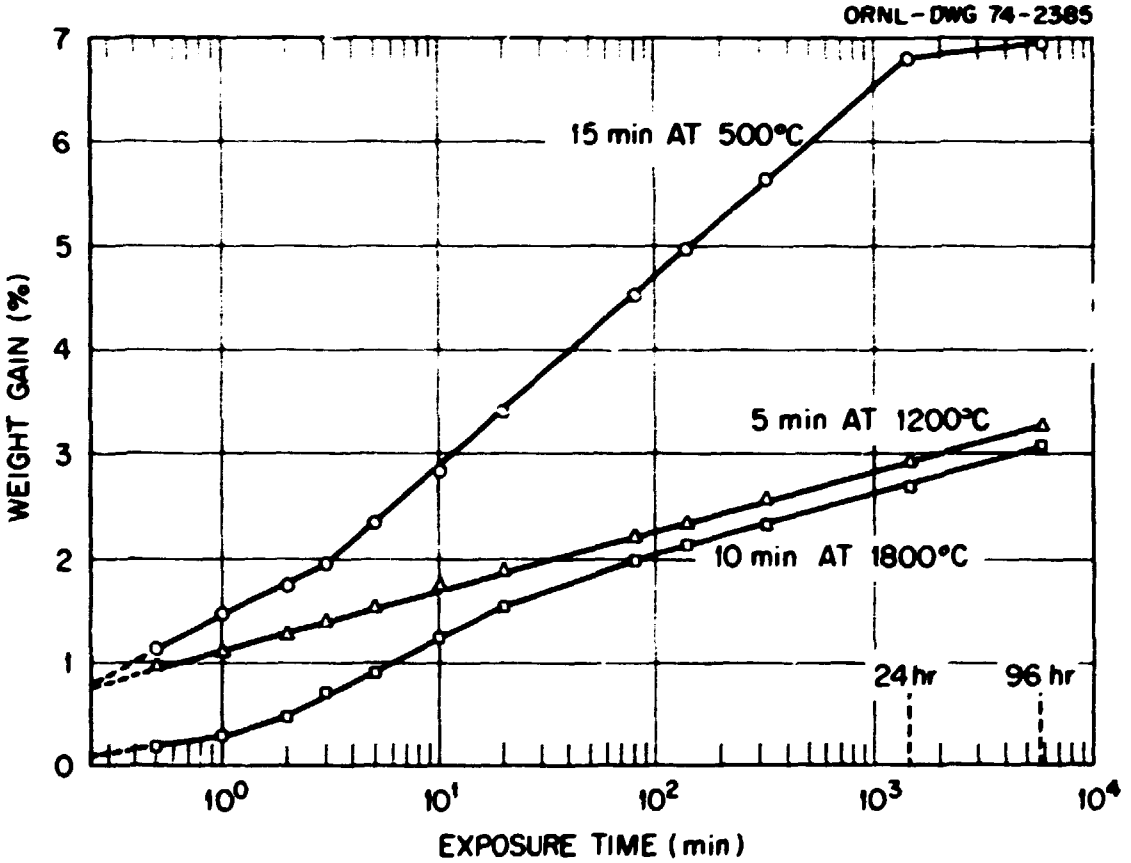

Fig. 30. Weight Gain of Uranium-Loaded Weak-Acid Resin, Heated at 2°C Min, Then as Indicated. One-gram Sample Exposed to Laboratory Air as Single Layer of Microspheres.

This appears to be related to surface area and surface reactivity rather than to chemical composition (e.g., partial conversion of oxide to carbide results in increased stability). The 1200 and 1800°C materials were reheated after exposure for 24 hr without loss of microsphere integrity, while the particles processed to only 500°C, exposed for 24 hr, and then reheated showed partial disintegration.

Another approach considered to circumvent the protective-atmosphere requirement was that of coating immediately after kernel processing. Particle-atmosphere reactivity would become a moot consideration if at least one layer of impermeable coating were applied to the particles before they are removed from the furnace. Consecutively carbonizing, converting, and coating in a single fabricating operation has been shown to be practicable, but product evaluation is complicated by the composite nature of this material.

CONCLUSIONS

1. Weak-acid, ion-exchange resins provide a versatile substance for fabrication of uranium-containing HTGR fuel kernels.

2. Two weak-acid resins, Amberlite IRC-72 and Duolite C-464, are suitable for use in HTGR fuel fabrication.

3. Kernel carbon content and bulk physical properties closely reflect the TGA behavior and are sensitive to heating rate through a narrow critical temperature range from about 350 to 440°C during the carbonization process.

4. The carbonization process can be optimized for both property control and process flow with a carbonization rate of approximately 2°C min through the critical range and the maximum practicable rate outside this range.

5. The conversion or carbothermic reduction of the UO_2 present after carbonization can be effected in a controlled manner in a fluidized bed at temperatures from 1500 to 1750°C.

6. The conversion rate is controlled by the rate of carbon monoxide removal and is predictable by thermodynamic calculations based on temperature and specific inert gas sweep rate.

7. Major phases present in partially converted material are UO_2 and UC_2. The amount of a minor phase, $UC_{1-x}O_x$, depends on conversion conditions.

8. A tendency of the particles to agglomerate during conversion can be effectively countered by controlling the carbonization rate to maximize carbon content, lowering temperature, increasing gas flow, or by buffer coating before conversion.

9. Duolite C-464 is superior to Amberlite IRC-72 in its resistance to sintering and agglomeration and is hence easier to control during conversion.

10. Uranium volatilization during processing is negligible except with extremely rapid carbonization.

11. Carbonized and/or converted kernels are sufficiently reactive to require a protective atmosphere and may ignite if exposed to air in bed depths greater than a few particle diameters.

ACKNOWLEDGMENTS

The authors would like to express their appreciation to the pioneering work done on the development of uranium-loaded weak-acid resin fuel by J. M. Leitnaker, C. B. Pollock, J. L. Scott, and M. D. Silverman. We wish to express our appreciation to C. Hamby, Jr., B. R. Chilcoat, and W. Smith who prepared the samples, B. R. Cavin for the x-ray analyses, W. R. Laing for the analytical chemistry, and W. J. Mason for radiography of the samples. The uranium-loaded resin particles were supplied by P. A. Haas and J. Shaffer of the Chemical Technology Division. We wish to acknowledge T. B. Lindemer for his many helpful

suggestions and W. P. Eatherly, W. J. Lackey, and J. A. Carpenter, Jr. for their assistance in planning the test program. The manuscript was edited by G. W. Griffith and prepared for reproduction by the Composition Section, Technical Publications Department.

REFERENCES

1. C. B. Pollock, J. L. Scott, and J. M. Leitnaker, "High Temperature Nuclear Reactor Fuel," U.S. Patent No. 3,856,622, Dec. 24, 1974.

2. P. A. Haas, "Loading a Cation-Exchange Resin with Uranyl Ions," U.S. Patent No. 3,800,023, March 26, 1974.

3. C. B. Pollock, "Resin Particle Development," *GCR-TU Programs Annual Progress Report, September 30, 1971*, ORNL-4760, pp. 96–100.

4. C. B. Pollock and M. D. Silverman, "Resin Particle Development," *GCR-TU Programs Annual Progress Report, Dec. 31, 1972*, ORNL-4911, pp. 90–95.

5. R. L. Beatty, "Carbonization and Coating of Fueled Resin Microspheres," presented at 76th Annual Meeting of Amer. Ceram. Soc., April 29, 1974, Chicago, Ill. Abstract in *Am. Ceram. Soc. Bull.* 53(4):363 (1974).

6. M. D. Silverman and C. B. Pollock, "Resin Fuel Particles for High Temperature Gas-Cooled Reactors," 11th Biennial Conf. Carbon, Gatlinburg, Tenn., June 4–8, 1973, Conf-730601, pp. 245–46.

7. R. L. Beatty and E. L. Long, Jr., "Preparation and Performance of Coated Particle Nuclear Fuels having UC_xO_y Kernels," Extended Abstract, 12th Biennial Conf. on Carbon, Pittsburg, Pa. July 28, 1975.

8. D. R. Johnson, W. J. Lackey, and J. D. Sease, "The Effects of Processing Variables on HTGR Fuel Kernels Fabricated from Uranium-Loaded Cation Exchange Resin," ORNL/TM-4989 (Aug. 1975).

9. J. L. Scott, J. A. Conlin, J. H. Coobs, W. P. Eatherly, F. J. Homan, and E. L. Long, Jr. "Performance of Candidate HTGR Fuels in Fuel Rod Irradiations in HFIR," ORNL/TM-4554 (Oct. 1974).

10. F. J. Homan, J. H. Coobs, R. L. Hamner, J. A. Conlin, B. H. Montgomery, E. L. Long, Jr. and J. L. Scott, "Irradiation Performance of HTGR Fuel Rods in HFIR Experiment HRB-3 and ETR Experiment P 13 N, ORNL/TM-4526 (Oct. 1974).

11. Amberlite IRC-72, Rohm and Haas Information Bulletin.

12. T. B. Lindemer, "Rate Controlling Factors in the Carbothermic Synthesis of Advanced Fuels," *Nucl Appl. and Tech.* 9, 711–15 (1970).

13. R. Bacon, p. 13 in *Chemistry and Physics of Carbon*, vol. 9, P. L. Walker and P. A. Thrower, ed., Dekker, New York, 1973.

14. B. D. Cullity, *Elements of X-Ray Diffraction*, p. 99, Addison-Wesley, Reading, Mass., 1956.

15. R. L. Pilloton, "Gas Flow Calculations for Fluidized Bed Coating of Nuclear Fuel Particles," ORNL-3639 (June 1964).

16. C. W. Nestor, ORNL Mathematics Division, unpublished data cited in ORNL-3639 (June 1964), p. 16.

17. R. D. Langeley, General Atomic, LaJolla, Calif., personal communication.